



Published in final edited form as:

SIAM J Appl Dyn Syst. 2008 ; 7(2): 609–649. doi:10.1137/070705842.

Mechanisms for Frequency Control in Neuronal Competition Models

Rodica Curtu[†], Asya Shpiro[‡], Nava Rubin[‡], and John Rinzel[§]

[†]Department of Mathematics, The University of Iowa, 14 MacLean Hall, Iowa City, IA 52242, and Transilvania University of Brasov, Romania (rodica-curtu@uiowa.edu)

[‡]Center for Neural Science, New York University, 4 Washington Place, New York, NY 10003 (asya@cns.nyu.edu, Nava.Rubin@nyu.edu)

[§]Courant Institute of Mathematical Sciences and Center for Neural Science, New York University, 4 Washington Place, New York, NY 10003 (rinzel@cns.nyu.edu)

Abstract

We investigate analytically a firing rate model for a two-population network based on mutual inhibition and slow negative feedback in the form of spike frequency adaptation. Both neuronal populations receive external constant input whose strength determines the system's dynamical state—a steady state of identical activity levels or periodic oscillations or a winner-take-all state of bistability. We prove that oscillations appear in the system through supercritical Hopf bifurcations and that they are antiphase. The period of oscillations depends on the input strength in a nonmonotonic fashion, and we show that the increasing branch of the period versus input curve corresponds to a release mechanism and the decreasing branch to an escape mechanism. In the limiting case of infinitely slow feedback we characterize the conditions for release, escape, and occurrence of the winner-take-all behavior. Some extensions of the model are also discussed.

Keywords

Hopf bifurcation; antiphase oscillations; slow negative feedback; winner-take-all; release and escape; binocular rivalry; central pattern generators

1. Introduction

Competition models have a long tradition in ecology and population biology (see, e.g., [22]). Typically, the competition involves negative interactions in the battle for a common resource. Eventually, one of the participant populations emerges as the winner eliminating the competitors. This framework has appeared in models of neuronal development where the competition is for synapse formation such as the development of neuromuscular connections for innervated muscle fibers and for the formation of ocular dominance columns and topographic maps (as reviewed in [35]). The notion of competition has also been applied in the modeling of various neuronal computational tasks. *Winner-take-all* behavior, when one neural population remains active and the others inactive indefinitely as a result of inhibitory interactions, has been proposed in models for short term memory and attention [13] or for the

selection and switching in the striatum of the basal ganglia under both normal and pathological conditions [15,21].

The winner-take-all steady state may persist for a long time but not indefinitely if some mechanism for slow fatigue or adaptation is at work. In this case one population may be dominant for a while, then another, and so on. Competition between, say, two neuronal populations, via reciprocal inhibition and slow adaptation underlies models for alternating rhythmic behavior in central pattern generators (CPGs) [11,32,6,33] and in perceptual bistability [17,37,24]. CPGs consist of neural circuits that drive alternately contracting muscle groups. Perceptual bistability refers to a class of phenomena in which a deeply ambiguous stimulus gives rise to two different interpretations that alternate over time, only one being perceived at any given moment. Slow adaptation may be implemented via a cellular mechanism (fatigue in the spike generation mechanism) or a negative feedback in the coupling (depression of the synaptic transmission mechanism). In some neuronal competition models the alternations may be irregular and caused primarily by noise, with adaptation playing a secondary role [30,10,24].

Both for CPGs and perceptual bistability the issue of oscillations' frequency or period detection (and eventually control) seems to be important. For example, a classical example of perceptual bistability is binocular rivalry whose properties were summarized in the so-called Levelt's propositions [19]. In binocular rivalry, a subject views an ambiguous stimulus in which each eye is presented with a drastically different image. Instead of perceiving a mixture of the two images, the subject reports (over a large range of stimulus conditions) an alternation between the two competing percepts; one image is perceived for a while (a few seconds), then the other, etc. Levelt's proposition IV (LP-IV) states that increasing the contrast of the rivaling images increases the frequency of percept switching, or, in other words, that dominance times of both perceived images decrease with equal increase of stimulus strength. Since 1968, binocular rivalry has been investigated intensively in other psychophysics experiments [2,25,20,1,28, 29,3], in experiments using fMRI techniques [34,26,38,18], and also in modeling studies [17, 37,10,24].

In a recent modeling paper, Shpiro et al. [31] show that for a class of competition models, the LP-IV type of dynamics occurs in fact only within a limited range of stimulus strength. Outside this range four other types of behavior were observed: (i) fusion at a very high level of activity, (ii) winner-take-all behavior, (iii) a region where dominance times increase with stimulus strength (as opposed to LP-IV), and then (iv) fusion again for very low levels of activity (see Figure 3F in section 2). These differences between experimental reports and theory have important implications, either predicting new possible dynamics in binocular rivalry or, if future experiments do not confirm them, pointing to the necessity for other types of models. Meanwhile, it is important to understand the sources or mechanisms that lead to the nonmonotonic dependence of oscillation period on the stimulus strength for this class of neuronal competition models. Our paper aims to investigate this issue.

We analyze a firing rate model in which competition between populations is a result of a combination of reciprocal inhibition and a slow negative feedback process. We prove that, as the input strength changes, oscillations appear in the system through a Hopf bifurcation and that they are antiphase. Due to the two time scales involved in the system there is a regime where periodic solutions take the form of relaxation-oscillators. Their period of oscillations depends nonmonotonically on the input strength, say, I : in a range of low values for I , the period increases with I , and we show that the dynamics is due to a *release* mechanism; on the other hand, in a range of higher values for I , the period decreases with I , and *escape* is the underlying mechanism (see section 4; we define release as the case when the switch in dominance during oscillation occurs due to a significant change in the response to an input to the dominant

population. On the contrary, escape corresponds to the case of a significant change in the input-output function for the suppressed population). For intermediate values of I , winner-take-all is possible and we explain how it appears. Then in section 5 we present some model modifications that allow for reducing, or even excluding, one of the escape and release regimes, thus leading to a monotonic period versus input curve.

2. The mathematical model

The model we investigate in this paper assumes a network architecture of two populations of neurons (Figure 1) that respond to two competing stimuli of equal strength:

$$\begin{aligned}\dot{u}_1 &= -u_1 + S(I - \beta u_2 - g a_1), \\ \dot{u}_2 &= -u_2 + S(I - \beta u_1 - g a_2), \\ \tau \dot{a}_1 &= -a_1 + u_1, \\ \tau \dot{a}_2 &= -a_2 + u_2.\end{aligned}\tag{2.1}$$

Variables u_j ($j = 1, 2$) measure short-time and spatially averaged firing rates of the two populations that inhibit each other. The system is nonlinear due to the gain function S ; it is the steady input-output function for the population and it has a sigmoid shape as in Figure 2A. The strength of inhibition is modeled by the positive parameter β , while I is the control parameter directly associated to the external stimulus strength (e.g., it grows with growing stimulus strength such as contrast). Each population is subject to a slow negative feedback process a_j such as spike frequency adaptation of positive strength g . Since variables a_j evolve in much slower time than u_j , the parameter τ takes large values, $\tau \gg 1$ (e.g., the time-scale for u_j is about 10 msec, while for a_j it is about 1000 msec).

Remark 2.1. *In general, firing-rate models like (2.1) include in the equation of u_j a nonlinear term of the form $S(I + a u_j - \beta u_k - g a_j)$. The product $a u_j$ is associated with the intrapopulation recurrent excitation. It is important to note that for neuronal competition model (2.1) we have disallowed recurrent excitation (taken $\alpha = 0$) in order to preclude an isolated population ($\beta = 0$) from oscillating on its own. This is a restriction imposed by experimental observations on binocular rivalry and other perceptual bistable phenomena.*

The nonlinear gain function S that appears in the differential equations for u_j is usually defined in neuronal models by

$$S(x) = \frac{1}{1 + e^{-r(x-\theta)}}\tag{2.2}$$

with positive r and real θ .

Function S is invertible with $F = S^{-1}$ a $C^\infty(0, 1)$ -function and $F'(u) = \frac{1}{ru(1-u)}$ (Figure 2B–C). Based on this example, we consider the following *assumptions* for with positive for the gain function S .

$S: \mathbf{R} \rightarrow (0, 1)$ is a differentiable, monotonically increasing function with $S(\theta) = u_0 \in (0, 1)$ and $\lim_{x \rightarrow -\infty} S(x) = 0$, $\lim_{x \rightarrow \infty} S(x) = 1$. Moreover, its first and second derivatives satisfy the conditions $\lim_{x \rightarrow \pm\infty} S'(x) = 0$, $S''(x) > 0$ for $x < \theta$, $S''(x) < 0$ for $x > \theta$, and $S''(\theta) = 0$, so S' has a maximum at θ .

As a consequence, S is invertible with $F = S^{-1} : (0, 1) \rightarrow \mathbf{R}$ monotonically increasing function such that $\lim_{u \rightarrow 0} F(u) = -\infty$, $\lim_{u \rightarrow 1} F(u) = \infty$, $F(u_0) = \theta$, and $\lim_{u \rightarrow 0} F'(u) \lim_{u \rightarrow 1} F'(u) = \infty$, $F''(u) < 0$ for $u \in (0, u_0)$, $F''(u) > 0$ for $u \in (u_0, 1)$, $F''(u_0) = 0$. Obviously, F' has a minimum value at u_0 which is $F'(u_0) = 1/S'(\theta)$.

Additionally we assume that F is a C^∞ -function on $(0, 1)$, or at least C^2 on $(0, 1)$ and C^∞ on $(0, 1) \setminus \{u_0\}$.

The typical graphs of function S and its corresponding F and F' are drawn in Figure 2A–C. We used the example (2.2) with parameter values $r = 10$ and $\theta = 0.2$; obviously in this case $S(\theta) = u_0 = 0.5$.

All the experiments that motivated our work report oscillatory phenomena with frequencies tightly connected to the stimulus strengths. Moreover, as Levelt [19] pointed out for binocular rivalry, those experiments show large ranges for stimulus strength where the corresponding oscillation periods/frequencies behave monotonically. What kind of possible mechanism is behind this type of dynamics is the question we will focus on in this paper.

Given the neuronal competition model (2.1), the goal is to examine the effect the parameter I has on the existence of oscillations and on their period. The system is a simplified version of an entire class of competition models that, as we found [31], share important dynamical features.

To illustrate those commonalities we draw in Figure 3A–E the timecourses of activity variables $u_1(t)$ and $u_2(t)$ for different values of control parameter I . Then we summarize the result in the bifurcation diagram of the period T versus I (Figure 3F). Other parameter values are fixed to $\beta = 1.1$, $g = 0.5$, $\tau = 100$, and S as in (2.2) with $r = 10$ and $\theta = 0.2$ (here $u_0 = 1/2$). The system (2.1) exhibits five possible types of behavior: for large values of I (region I in Figure 3F) both populations are active at identically high levels (Figure 3A); the timecourses of $u_1(t)$ and $u_2(t)$ tend to a stable steady state larger than u_0 . As I decreases (region II, Figure 3F) the system starts oscillating with $u_1(t)$ and $u_2(t)$ alternatively on and off (Figure 3B); in this region the period of oscillation decreases with increasing input strength. At intermediate values of I a winner-take-all kind of behavior is observed (region III, Figure 3F); depending on the choice of initial conditions, one of the two populations is active indefinitely, while the other one remains inactive (Figure 3C). Decreasing I even more (region IV, Figure 3F) the neuronal model becomes oscillatory again (Figure 3D) with u_1 and u_2 competing for the active state; however, for this range of parameter the oscillation period T increases with input value I —an opposite behavior to that observed in region II. Last, for small values of stimulus strength (region V, Figure 3F) both populations remain inactive at identically low level firing rates (Figure 3E); the timecourses of $u_1(t)$ and $u_2(t)$ tend to a stable steady state less than u_0 .

To further characterize system (2.1)'s dynamics as the input value I is varied, we also construct the local bifurcation diagram of amplitude response u_1 to I (Figure 3G). For the parameter ranges I and V the trajectories are attracted to a stable fixed point satisfying the $\tilde{u}_1 = \tilde{u}_2$ condition (thick line in Figure 3G). This fixed point becomes unstable (dashed line) in regions II, III, and IV, where the attractor is replaced by either a stable limit cycle (regions II and IV: branched filled-circle curves corresponding to the maximum and minimum amplitudes during rivalry oscillations) or another stable fixed point with $\tilde{u}_1 \neq \tilde{u}_2$ (region III). Due to the symmetry in the equations of (2.1) whenever $(\tilde{u}_1, \tilde{u}_2, \tilde{a}_1, \tilde{a}_2)$ is an equilibrium point, $(\tilde{u}_2, \tilde{u}_1, \tilde{a}_2, \tilde{a}_1)$ is as well. The local bifurcation diagram suggests the existence of some Hopf and pitchfork bifurcations in the model that we will further investigate in section 3.

There is another common feature of many neuronal competition models based on reciprocal inhibition architecture with slow negative feedback in the form of spike frequency adaptation and/or synaptic depression [31]: the absence of the winner-take-all behavior when inhibition strength β is sufficiently small. As we illustrate in Figure 3H–I for $\beta = 0.75$ (all other parameters are the same as above), the winner-take-all regime at intermediate I disappears. However, the dependency of period T on stimulus strength remains nonmonotonic.

An intriguing question is: What are the neuronal mechanisms underlying the two distinct dynamics—one of increasing period with increase of stimulus strength (for smaller values of input), and one of decreasing period (for larger values)? This issue is discussed in section 4 and then extended in section 5.

Our general goal is to understand and possibly to analytically characterize the numerical results obtained for this specific competition model (2.1). Consequently, as already pointed out, this step will help us understand the typical behavior of an entire class of neuronal competition models.

3. Oscillatory antiphase solutions and local analysis

In this section we use methods from local bifurcation theory [14,16] to prove the existence of periodic solutions $(u_1(t), u_2(t), a_1(t), a_2(t))$ for the two-population network (2.1). We also show that the main variables u_1 and u_2 oscillate in antiphase, therefore competing for the ON/active state.

The bifurcation diagrams obtained numerically in section 2 suggest the existence of an equilibrium point satisfying $u_1 = u_2$ no matter the value of parameter I . Let us now investigate system (2.1) theoretically.

All equilibria satisfy the conditions $u_1 = S(I - \beta u_2 - g a_1)$, $u_2 = S(I - \beta u_1 - g a_2)$, $a_1 = u_1$, and $a_2 = u_2$ that are equivalent (due to the invertibility of S) to $F(u_1) = I - \beta u_2 - g a_1$, $F(u_2) = I - \beta u_1 - g a_2$, and $a_1 = u_1$, $a_2 = u_2$. Looking for a particular type of equilibrium point, that is, for points with $u_1 = u_2$, we obtain the equation $I = H(u)$ with H defined by

$$H: (0, 1) \rightarrow \mathbf{R}, \quad H(u) \stackrel{\text{def}}{=} F(u) + (\beta + g)u. \quad (3.1)$$

Since F is monotonically increasing on $(0, 1)$ with vertical asymptotes $\lim_{u \rightarrow 0} F(u) = -\infty$ and $\lim_{u \rightarrow 1} F(u) = \infty$, (3.1) has a unique solution $u_I \in (0, 1)$ for any real value of the parameter I . Moreover, from the identity $I = F(u_I) + (\beta + g)u_I$ we compute

$$\frac{du_I}{dI} = \frac{1}{\beta + g + F'(u_I)}, \quad (3.2)$$

so a decrease in I leads to a decrease in u_I with $\lim_{I \rightarrow \infty} u_I = 1$ and $\lim_{I \rightarrow -\infty} u_I = 0$.

The neuronal competition model (2.1) always possesses an equilibrium of the type (u_I, u_I, u_I, u_I) . Its stability properties are then defined by the linearized system $dY/dt = \mathcal{A}Y$, $Y = (u_1 - u_I, u_2 - u_I, a_1 - u_I, a_2 - u_I)^T$, where $()^T$ stays for the transpose, and matrix

$$\mathcal{A} = \begin{pmatrix} -1 & -\beta/F'(u_I) & -g/F'(u_I) & 0 \\ -\beta/F'(u_I) & -1 & 0 & -g/F'(u_I) \\ 1/\tau & 0 & -1/\tau & 0 \\ 0 & 1/\tau & 0 & -1/\tau \end{pmatrix}.$$

This form of the matrix relies on the equality $S'(I - \beta u_2 - g a_1) = S'(F(u_1)) = S'(S^{-1}(u_1)) = 1/(S^{-1})'(u_1) = 1/F'(u_1)$, which is true at the equilibrium point.

The characteristic equation of \mathcal{A} takes the form

$$\left[(\lambda + 1) \left(\lambda + \frac{1}{\tau} \right) + \frac{g}{\tau F'(u_I)} \right]^2 - \left[\frac{\beta}{F'(u_I)} \left(\lambda + \frac{1}{\tau} \right) \right]^2 = 0.$$

As a difference of squares it can be decomposed into two quadratic equations: the first is

$$\lambda^2 + \lambda \left(1 + \frac{1}{\tau} + \frac{\beta}{F'(u_I)} \right) + \frac{1}{\tau} \left(1 + \frac{g + \beta}{F'(u_I)} \right) = 0,$$

so two eigenvalues of the matrix \mathcal{A} , say, λ_1 and λ_2 , have negative real part no matter the value of parameter I . The other eigenvalues λ_3 and λ_4

satisfy the second quadratic equation $\lambda^2 + \lambda \left(1 + \frac{1}{\tau} - \frac{\beta}{F'(u_I)} \right) + \frac{1}{\tau} \left(1 + \frac{g - \beta}{F'(u_I)} \right) = 0$, and their real part can change sign when I is varied.

For $|I|$ sufficiently large, u_I is close to either zero or one, keeping $F'(u_I)$ larger than both

$\beta / \left(1 + \frac{1}{\tau} \right)$ and $\beta - g$ (see Figure 2C); the corresponding equilibrium point (u_b, u_b, u_b, u_I) is asymptotically stable.

There are two ways this equilibrium point can lose stability: either through a pair of purely

imaginary eigenvalues $\lambda_{3,4} = \pm i\omega$ at $F'(u_I) = \beta / \left(1 + \frac{1}{\tau} \right)$ or through a zero eigenvalue $\lambda_3 = 0$, $\lambda_4 < 0$ at $F'(u_I) = \beta - g$. Which of these two cases occurs first depends on the relationship

between $\beta / \left(1 + \frac{1}{\tau} \right)$ and $\beta - g$: if $\beta / \left(1 + \frac{1}{\tau} \right) > \beta - g$, i.e., $\beta/g < \tau + 1$, then the eigenvalues λ_3, λ_4 change the sign of their real part from negative to positive by crossing the imaginary axis ($\lambda_{3,4} = \pm i\omega$); if $\beta/g > \tau + 1$, then the case $\lambda_3 = 0, \lambda_4 < 0$ is encountered first.

At this point we remind the reader of our assumption of a large time constant value τ . (The competition between the populations in the network comes from the combination of two important ingredients: reciprocal inhibition and the addition of a slow negative feedback process.) Therefore, it makes sense to situate ourselves in the case of $\beta/g \ll \tau$, which implies

$$\beta < g(\tau + 1). \tag{3.3}$$

Inequality (3.3) can be interpreted as a feature of the neuronal competition model to be rather (adaptation) feedback-dominated than (inhibitory) coupling-dominated.

We will assume in the following that parameters g and τ are fixed and that β is chosen such that (3.3) is true.

Another observation is that the graph of F' has a *well-like* shape with positive minimum at $1/S'(\theta)$ as in Figure 2C. Consequently the straight horizontal line $y = \beta / \left(1 + \frac{1}{\tau}\right)$ intersects it twice (if $\beta / \left(1 + \frac{1}{\tau}\right) > 1/S'(\theta)$), once (for the equality), or not at all (if $\beta / \left(1 + \frac{1}{\tau}\right) < 1/S'(\theta)$). As observed in numerical simulations, in order for the system to oscillate, a sufficiently large inhibition strength has to be considered. Mathematically that reduces to

$$\beta > \frac{1 + 1/\tau}{S'(\theta)}. \tag{3.4}$$

Thus we are able to characterize the stability of the equilibrium (u_I, u_I, u_I, u_I) .

Theorem 3.1. *The dynamical system (2.1) has a unique equilibrium point with $u_1 = u_2$, say, $\mathbf{e}_I = (u_I, u_I, u_I, u_I)$, for any real I . The value u_I increases monotonically with I and belongs to the interval $(0, 1)$.*

Let us assume that the adaptation-dominance condition (3.3) is true.

- i. If $\beta < \frac{1 + 1/\tau}{S'(\theta)}$, then \mathbf{e}_I is asymptotically stable for all $I \in \mathbf{R}$.
- ii. If $\beta > \frac{1 + 1/\tau}{S'(\theta)}$ then there exist exactly two values $u_{hb}^*, u_{hb}^{**} \in (0, 1)$ such that $u_{hb}^* < u_0 < u_{hb}^{**}$ and

$$F'(u_{hb}^*) = F'(u_{hb}^{**}) = \frac{\beta}{1 + \frac{1}{\tau}}. \tag{3.5}$$

The equilibrium point \mathbf{e}_I is asymptotically stable for all $I \in (-\infty, I_{hb}^*) \cup (I_{hb}^{**}, \infty)$ and unstable for $I \in (I_{hb}^*, I_{hb}^{**})$, where $I_{hb}^* = H(u_{hb}^*)$, $I_{hb}^{**} = H(u_{hb}^{**})$ defined by (3.1). At I_{hb}^* and I_{hb}^{**} the stability is lost through a pair of purely imaginary eigenvalues.

Proof.

- i. Since $\beta - g < \beta / \left(1 + \frac{1}{\tau}\right) < 1/S'(\theta) = \min(F')$, all eigenvalues of the linearized system about \mathbf{e}_I have negative real part.
- ii. The conclusion is based on the properties of F' , which decreases on interval $(0, u_0)$ and increases on $(u_0, 1)$ with $F'(u_0) = \min(F')$. The sum $\lambda_3 + \lambda_4$ changes sign from negative to positive when I increases through I_{hb}^* and then back from positive to negative when passing through I_{hb}^{**} . For $I \in (I_{hb}^*, I_{hb}^{**})$ at least one real part of λ_3 and λ_4 is positive, so \mathbf{e}_I is unstable. At $I = I_{hb}^*$ and $I = I_{hb}^{**}$ we have $\lambda_{3,4} = \pm i\omega$. For all other values of I we have $\lambda_3 + \lambda_4 < 0$, $\lambda_3\lambda_4 > 0$; so \mathbf{e}_I is asymptotically stable.

Since the equilibrium point \mathbf{e}_I becomes unstable through a pair of purely imaginary eigenvalues as I crosses the values I_{hb}^* and I_{hb}^{**} we expect to find there two Hopf bifurcation points. Indeed, in section 3.1 we prove the existence of a supercritical Hopf bifurcation at both I_{hb}^* and I_{hb}^{**} and, as a consequence, the existence of stable oscillatory solutions for system (2.1).

3.1. Normal form for the Hopf bifurcation

In the following we assume that both inequalities (3.3) and (3.4) are true; that is, we take the coupling in (2.1) to be sufficiently strong but still adaptation-dominated.

Let us use the notation I^* for any of the critical values I_{hb}^* and I_{hb}^{**} and similarly the notation u^* for $u^* \in \{u_{hb}^*, u_{hb}^{**}\}$. Then the linearization matrix \mathcal{A} at u^* becomes

$$\mathcal{A}_0 = \begin{pmatrix} -1 & -\left(1+\frac{1}{\tau}\right) & -\frac{g}{\beta}\left(1+\frac{1}{\tau}\right) & 0 \\ -\left(1+\frac{1}{\tau}\right) & -1 & 0 & -\frac{g}{\beta}\left(1+\frac{1}{\tau}\right) \\ \frac{1}{\tau} & 0 & -\frac{1}{\tau} & 0 \\ 0 & \frac{1}{\tau} & 0 & -\frac{1}{\tau} \end{pmatrix},$$

and it has eigenvalues $\lambda_{1,2}$ with $\text{Re}(\lambda_{1,2}) < 0$ and $\lambda_{3,4} = \pm i\omega$,

$$\omega = \frac{1}{\tau} \sqrt{\frac{g(\tau+1)}{\beta} - 1}. \tag{3.6}$$

The system (2.1) has an equilibrium \mathbf{e}_I for any $I \in \mathbf{R}$; we translate \mathbf{e}_I to the origin with the change of variables $v_j = u_j - u_I$, $b_j = a_j - u_I$ ($j = 1, 2$) and obtain a system topologically equivalent to (2.1),

$$\begin{aligned} \dot{v}_1 &= -v_1 + S(F(u_I) - \beta v_2 - gb_1) - u_I, \\ \dot{v}_2 &= -v_2 + S(F(u_I) - \beta v_1 - gb_2) - u_I, \\ \tau \dot{b}_1 &= -b_1 + v_1, \\ \tau \dot{b}_2 &= -b_2 + v_2. \end{aligned} \tag{3.7}$$

Near u^* , $u^* \neq u_0$, we expand the nonlinear terms in (3.7) with respect to u_I and obtain for v_1 (and similarly for v_2) an equation of the form

$$\dot{v}_1 = -v_1 - S'(F(u_I)) \cdot (\beta v_2 + gb_1) + \frac{1}{2} S''(F(u_I)) \cdot (\beta v_2 + gb_1)^2 - \frac{1}{6} S'''(F(u_I)) \cdot (\beta v_2 + gb_1)^3 + h.o.t. \tag{3.8}$$

Here *h.o.t.* means the *higher order terms*. The parameter value I^* is a possible Hopf bifurcation, so we consider small perturbations about it and about the solution u^* . That is, we take

$$I - I^* = \varepsilon^2 \alpha, \quad V(t) = \varepsilon V_0(t) + \varepsilon^2 V_1(t) + \varepsilon^3 V_2(t) + \dots, \tag{3.9}$$

where α is the bifurcation parameter and $V = (v_1, v_2, b_1, b_2)^T$.

The expansions of the coefficients $S^{(k)}(F(u_I))$, $k = 1, 2, 3, \dots$, with respect to take the form

$$S'(F(u_I)) = \left(1 + \frac{1}{\tau}\right) / \beta + \alpha A \varepsilon^2 + \mathcal{O}(\varepsilon^4), \quad S''(F(u_I)) = B + \mathcal{O}(\varepsilon^2) \quad \text{and} \quad S'''(F(u_I)) = D + \mathcal{O}(\varepsilon^2),$$

where A , B , and D are defined by

$$A = -\frac{F''(u^*)}{F'(u^*)^2(\beta + g + F'(u^*))}, B = -\frac{F''(u^*)}{F'(u^*)^3}, D = \frac{3F''(u^*)^2 - F'(u^*) \cdot F'''(u^*)}{F'(u^*)^5} \tag{3.10}$$

(see Appendix A for more details). Let us introduce the following notation: for two vectors $U = (v_1, v_2, b_1, b_2)^T$ and $W = (w_1, w_2, c_1, c_2)^T$ we define first the quantities $\tilde{v}_{ij} = \beta v_j + g b_i$, $\tilde{w}_{ij} = \beta w_j + g c_i$ and then, using the scalars from (3.10), we define the operators

$$L_0 U = \frac{dU}{dt} - \mathcal{A}_0 U, \quad \Lambda U = -\alpha A(\tilde{v}_{12}, \tilde{v}_{21}, 0, 0)^T, \\ \mathcal{B}(U, W) = \frac{\beta}{2}(\tilde{v}_{12}\tilde{w}_{12}, \tilde{v}_{21}\tilde{w}_{21}, 0, 0)^T, \quad C(U, U, U) = -\frac{\beta}{6}(\tilde{v}_{12}^3, \tilde{v}_{21}^3, 0, 0)^T.$$

Then based on (3.8), (3.9), and (3.10), we write system (3.7) as

$$L_0 V_0 = \varepsilon [\mathcal{B}(V_0, V_0) - L_0 V_1] + \varepsilon^2 [C(V_0, V_0, V_0) + 2\mathcal{B}(V_0, V_1) + \Lambda V_0 - L_0 V_2] + \mathcal{O}(\varepsilon^3).$$

The construction of the normal form relies on an algorithm that we describe in Appendix A (see also [4, 5] for a similar approach) and that involves tedious calculations; we present here only the main result.

Theorem 3.2. *Let us assume that conditions (3.3) and (3.4) are true (sufficiently strong coupling and adaptation-dominated system), and take $I^* \in \{I_{hb}^*, I_{hb}^{**}\}, u^* \in \{u_{hb}^*, u_{hb}^{**}\}$ as in normal Theorem 3.1. Then the system (2.1) has in the neighborhood of I^* the normal form*

$$\dot{z} = A\varphi(I - I^*)z - \mathcal{L}z^2 \bar{z}, \tag{3.11}$$

where z is a complex variable and

$$\mathcal{L} = 4\tau^2 \omega^2 \frac{|\varphi|^2}{|\psi|^2} \varphi \psi \left(\frac{\beta + g}{2} + i\beta\omega\tau \right) B^2 + 2\tau^2 \omega^2 |\varphi|^2 \varphi \left(\frac{2(\beta + g)}{1 + (\frac{g}{\beta} + 1)(1 + \frac{1}{\tau})} B^2 - D \right)$$

with $\varphi = \frac{\beta}{2} + i\frac{g - \beta}{2\tau\omega}$, $\psi = 2 - \frac{3g}{\beta} + \frac{1}{\tau} \left(5 - \frac{3g}{\beta} \right) - 4i\omega(\tau + 1)$ and A, B, D as in (3.10).

In order to show that I_{hb}^* and I_{hb}^{**} are supercritical Hopf bifurcation points, we need to check that the coefficient of $z^2 \bar{z}$ has negative real part, i.e., that $\text{Re}(\mathcal{L}) > 0$.

As we prove in the appendix, for our range of parameters β, g , and τ , the first term in \mathcal{L} has indeed positive real part (see (A.3)); on the other hand, the real part of the second term (see (A.4)) is larger than

$$\beta\tau^2 \omega^2 |\varphi|^2 B^2 F'(u^*) \left(\frac{F'(u^*) F''(u^*)}{F''(u^*)^2} - 2 \right).$$

Remark 3.1. The inverse of function S defined by (2.2) satisfies the condition

$$F'(u^*)F''(u^*) > 2F''(u^*)^2. \tag{3.12}$$

Moreover, the inequality (3.12) is true not only for u^* but for all $u \in (0, 1)$.

We use this observation to state our next result.

Theorem 3.3. Let us assume the same hypotheses as in Theorem 3.2. Given at $u^* \in \{u_{hb}^*, u_{hb}^{**}\}$ the property (3.12) for the gain function S , the input value I^* is a supercritical Hopf bifurcation point for system (2.1). The stable limit cycle occurs on the left side of I_{hb}^{**} (that is, for sufficiently close $I < I_{hb}^{**}$) and on the right side of I_{hb}^* ($I > I_{hb}^*$).

Proof. The Hopf bifurcation is supercritical since $\text{Re}(\mathcal{L}) > 0$ in the normal form; the nondegeneracy condition is $\text{Re}(A\varphi) = A\beta/2 \neq 0$.

The sign of A is opposite to the sign of $F''(u^*)$, so $A > 0$ for u_{hb}^* and $A < 0$ for u_{hb}^{**} . Consequently the sign of $\text{Re}(A\varphi(I - I^*))$ that shows the direction of limit cycle bifurcation is positive for $I > I_{hb}^*$ and $I < I_{hb}^{**}$.

Remark 3.2. It is possible to obtain supercritical Hopf bifurcation points for other types of gain-function than (3.12), as long as $\text{Re}(\mathcal{L})$ has positive value. When (3.12) is not valid, the sign of $\text{Re}(\mathcal{L})$ will be computed directly from the definition formula of \mathcal{L} .

3.2. Antiphase oscillations

The stable limit cycle that exists in the neighborhood of the bifurcation points I_{hb}^* (for $I > I_{hb}^*$) and I_{hb}^{**} (for $I < I_{hb}^{**}$) is a periodic solution $L_1(t) = (u_1(t), u_2(t), a_1(t), a_2(t))$ of period, say, T . Due to the symmetry of the system (2.1) with respect to the group $\Gamma = \{\mathbf{1}_4, \gamma\}$ where $\mathbf{1}_4$ is the unitary 4-by-4 matrix and

$$\gamma = \begin{pmatrix} 0 & 1 & 0 & 0 \\ 1 & 0 & 0 & 0 \\ 0 & 0 & 0 & 1 \\ 0 & 0 & 1 & 0 \end{pmatrix},$$

$L_2(t) = \gamma L_1(t) = (u_2(t), u_1(t), a_2(t), a_1(t))$ is also a periodic solution for (2.1). L_2 results automatically from solution L_1 by relabeling the two network's populations. Moreover, it belongs to the same neighborhood of the equilibrium point as L_1 does.

Since the limit cycle born through the Hopf bifurcation is unique, the corresponding phase space trajectories of L_1 and L_2 coincide. Therefore, there exists a phase shift $\alpha_0 \in [0, T)$ such that $L_2(t) = L_1(t + \alpha_0)$. This implies $u_2(t) = u_1(t + \alpha_0)$ and $u_1(t) = u_2(t + \alpha_0)$, i.e., $u_1(t) = u_1(t + 2\alpha_0)$ for all real t [12]. The phase shift α_0 needs to satisfy $\alpha_0 = kT/2$ with k an integer, so k is either $k = 0$ or $k = 1$. If $k = 0$, the two populations in the network will oscillate in synchrony. If $k = 1$, we have $u_2(t) = u_1(t + T/2)$ and $a_2(t) = a_1(t + T/2)$, which means an antiphase oscillation.

Let us assume for the moment that $k = 0$. Then $U(t) = (u_1(t), u_1(t), a_1(t), a_1(t))$ is a periodic solution of (2.1), and, as a consequence, $(u_1(t), a_1(t))$ is a periodic solution of the two-dimensional system

$$\dot{u}_1 = -u_1 + S(I - \beta u_1 - g a_1), \quad \tau \dot{a}_1 = -a_1 + u_1.$$

This contradicts Bendixon’s criterion: the expression

$$\frac{\partial}{\partial u_1} (-u_1 + S(I - \beta u_1 - g a_1)) + \frac{\partial}{\partial a_1} \left(-\frac{a_1}{\tau} + \frac{u_1}{\tau} \right) = -1 - \beta S' (I - \beta u_1 - g a_1) - \frac{1}{\tau}$$

is always negative, so our initial assumption should be false.

Excluding the first case, the limit cycle has to be an antiphase solution of (2.1): the two populations compete indeed for the active state (see, for example, Figure 3B or 3D).

We state our conclusion in the following theorem.

Theorem 3.4. *Let us assume that conditions (3.3) and (3.4) are true and the coefficient \mathcal{L} in the normal form (3.11) has positive real part. Then the stable limit cycle obtained at the supercritical Hopf bifurcation (as I crosses either I_{hb}^* or I_{hb}^{**}) corresponds to an antiphase oscillation: the limit cycle of period T satisfies $u_2(t) = u_1(t + T/2)$ and $a_2(t) = a_1(t + T/2)$ for any real t .*

3.3. Multiple equilibria for large enough inhibition

Our local analysis shows how stable oscillations occur in system (2.1)—through a Hopf bifurcation. The uniform equilibrium point \mathbf{e}_I has four eigenvalues, λ_1 and λ_2 with negative real part independent of I ($\text{Re}(\lambda_{1,2}) < 0$), and λ_3 and λ_4 that can cross the imaginary axis. Besides Hopf, another type of local bifurcation appears in (2.1) when one of the eigenvalues λ_3, λ_4 takes zero value, that is, when $F'(u_I) = \beta - g$. Because of the system’s symmetry we expect it to be a pitchfork bifurcation.

Numerical simulations of system (2.1) reveal indeed the existence of additional equilibrium points. However, they exist for stronger (Figure 3G, $\beta = 1.1$) but not for weaker inhibition (Figure 3I, $\beta = 0.75$). We explain analytically how that happens.

Theorem 3.5.

- i. *If $\beta - g < 1/S'(\theta)$, then the dynamical system (2.1) has a unique equilibrium point for all real I and this is $\mathbf{e}_I = (u_p, u_f, u_f, u_p)$.*
- ii. *For strong inhibition,*

$$\beta - g > 1/S'(\theta), \tag{3.13}$$

there are exactly two values, say, $u_{pf}^, u_{pf}^{**} \in (0, 1)$ such that $u_{pf}^* < u_0 < u_{pf}^{**}$ and*

$$F'(u_{pf}^*) = F'(u_{pf}^{**}) = \beta - g. \tag{3.14}$$

At $I_{pf}^ = H(u_{pf}^*)$ and $I_{pf}^{**} = H(u_{pf}^{**})$ defined by (3.1), the equilibrium point \mathbf{e}_I has a zero eigenvalue.*

Proof. The condition that characterizes the equilibrium points of (2.1) is equivalent to $G(u_1) = G(u_2) = I - \beta(u_1 + u_2)$, where we define G by $G(u) = F(u) + (g - \beta)u$, $u \in (0, 1)$. We have $\lim_{u \rightarrow 0} G(u) = -\infty$, $\lim_{u \rightarrow 1} G(u) = \infty$, and $G'(u) = F'(u) + g - \beta \geq F'(u_0) + g - \beta = 1/S'(\theta) + g - \beta$. Obviously, based on hypothesis (i), we have $G'(u) > 0$. Therefore, G is a monotonically increasing function; so it is injective, and the conclusion follows immediately. Statement (ii) results from the shape of F' .

By constructing the normal form of the system around the bifurcation point I_{pf}^* or I_{pf}^{**} , we prove the existence of a subcritical pitchfork bifurcation. Therefore, in the neighborhood of I_{pf}^* or I_{pf}^{**} the system (2.1) has multiple (three) equilibria. However, since the pitchfork is subcritical, the two newly born equilibrium points are unstable. In the four-dimensional eigenspace they actually possess two unstable modes (see Remark 3.4).

In some cases these nonuniform equilibria (having $u_1 \neq u_2$) might change their stability for I between I_{pf}^* and I_{pf}^{**} . Depending on the initial condition a trajectory will be attracted either to the fixed point with $u_1 > u_2$ or to that with $u_1 < u_2$, so one population is dominant and the other is suppressed forever. We call this type of dynamics in (2.1) *winner-take-all behavior*. The issue of the existence of the winner-take-all regime will be discussed separately in section 4.2. In this section we focus only on the mechanism that introduces additional equilibrium points to system (2.1).

Theorem 3.6. *Let us assume $\beta / \left(1 + \frac{1}{\tau}\right) > \beta - g > 1/S'(\theta)$ and take $I^\circ \in \{I_{pf}^*, I_{pf}^{**}\}$, $u^\circ \in \{u_{pf}^*, u_{pf}^{**}\}$ as in (3.14), $I^\circ = F(u^\circ) + (\beta + g)u^\circ$. Then the system (2.1) has in the neighborhood of I° the normal form*

$$\dot{z} = \frac{(I - I^\circ)F''(u^\circ)}{2\beta[g(\tau+1) - \beta]}z + \frac{(\beta - g)^2}{6[g(\tau+1) - \beta]} \left(F'(u^\circ)F'''(u^\circ) - \frac{3}{2}F''(u^\circ)^2 + \frac{3g}{2\beta} \right) z^3. \tag{3.15}$$

Moreover, if the gain function S satisfies (3.12) at $u^\circ \in \{u_{pf}^*, u_{pf}^{**}\}$, then I° is a subcritical pitchfork bifurcation point for the system (2.1). Two additional unstable equilibrium points occur on the left side of I_{pf}^{**} ($I < I_{pf}^{**}$) and on the right side of I_{pf}^* ($I > I_{pf}^*$).

Proof. The construction of the normal form is sketched in Appendix B. Since (3.12) is true, the coefficient of z^3 in the normal form is positive and the pitchfork is subcritical. Additional equilibrium points appear for $(I - I^\circ)F''(u^\circ) < 0$ with $F''(u^\circ)$ negative at u_{pf}^* and positive at u_{pf}^{**} .

Remark 3.3. In case of adaptation-dominated systems (when condition (3.3) or,

equivalently, $\beta / \left(1 + \frac{1}{\tau}\right) > \beta - g$ is true) we conclude the following: (1) for weak inhibition

$\beta - g < \beta / \left(1 + \frac{1}{\tau}\right) < 1/S'(\theta)$ system (2.1) has a unique equilibrium point \mathbf{e}_I which is asymptotically stable for all I ; (2) for some intermediate value of inhibition

$\beta - g < 1/S'(\theta) < \beta / \left(1 + \frac{1}{\tau}\right)$, the system still has a unique equilibrium point for all I but this becomes unstable in the interval (I_{hb}^*, I_{hb}^{**}) . However in order to obtain this case we need to

properly adjust the maximum gain to the adaptation parameters (i.e., we need $S'(\theta) > 1/$

(τg)); (3) for strong inhibition $(1/S'(\theta) < \beta - g < \beta / (1 + \frac{1}{\tau}))$, additional equilibrium points occur in system (2.1) for $I > I_{pf}^*$ and $I < I_{pf}^{**}$

Remark 3.4. In case of strong inhibition and adaptation-dominated system we obtain

$$u_{hb}^* < u_{pf}^* < u_0 < u_{pf}^{**} < u_{hb}^{**} \text{ and}$$

$$I_{hb}^* < I_{pf}^* < I_0 < I_{pf}^{**} < I_{hb}^{**}.$$

(Note that $I_0 = H(u_0)$ is independent of β .) At each I between I_{hb}^* and I_{hb}^{**} the equilibrium point \mathbf{e}_1 has at least one eigenvalue of positive real part. In fact for $I \in (I_{hb}^*, I_{pf}^*) \cup (I_{hb}^{**}, I_{pf}^{**})$ it has exactly two eigenvalues with positive real part and for $I \in (I_{pf}^*, I_{pf}^{**})$ it has only one eigenvalue with positive real part. Due to the multidimensionality of the eigenspace, at I_{pf}^* and I_{pf}^{**} the equilibrium \mathbf{e}_1 does not actually change its stability (even if an eigenvalue takes zero value). Instead two new (nonuniform) equilibria are born (e.g., Figure 3G). The two nonuniform equilibria inherit the number of unstable modes from their “parent”-fixed point, which means they have exactly two unstable modes.

As we see, condition (3.13) is necessary but not sufficient to obtain a winner-take-all behavior in system (2.1). In section 4.2, equations (4.11) and (4.10), we will determine the minimum value of β for which winner-take-all exists (β_{wta}) and the corresponding values I_w^* , I_w^{**} where transition from oscillation to winner-take-all dynamics takes place. We summarize all these results in Figure 4 by drawing the bifurcation diagram in the parameter plane (I, β) .

4. Release, escape, and winner-take-all mechanisms in neuronal competition models

As we mentioned in section 1, some common features are observed for a large class of neuronal competition models based on mutual inhibition and slow negative feedback process. An important example is the nonmonotonic dependency of the rivalry-oscillation’s period T on the stimulus strength I : in a range of small values for I the period increases with input strength; however, there exists another range for I , at larger values, where the period decreases with stimulus strength. These two dynamical regimes are usually separated by another one that is nonoscillatory; it occurs for sufficiently strong inhibition and corresponds to winner-take-all behavior (see Figures 3F and 3H).

The goal of this section is to characterize the underlying mechanisms of the above dynamical scheme. We aim to understand what causes the two opposite rivalry dynamics: as we will see, a *release* kind of mechanism is associated with the increasing branch of the T versus I curve (region IV in Figure 3F); on the other hand, for the decreasing branch of the I - T curve (region II in Figure 3F), an *escape* mechanism is responsible.

The terms *release* and *escape* were previously introduced by [36] for inhibition-mediated rhythmic patterns in thalamic model neurons and then extended and refined by [32] for Morris–Lecar equations. Most cases include an autocatalytic process either intrinsic by voltage-gated persistent inward currents or synaptic by intrapopulation recurrent excitation. In neuronal competition model (2.1) mutual inhibition plays the role of autocatalysis: one population inhibits the network partner that inhibited it; thus the combination of these two negative factors

has a positive effect on its own activity. Rhythmicity is obtained due to a fast positive feedback (disinhibition) and a slow negative feedback process. The slow negative feedback process can be either an intrinsic property of the neuronal populations (e.g., spike frequency adaptation as in (2.1)) or a property of the inhibitory connections between them (e.g., synaptic depression). A simplified model similar to (2.1) but with synaptic depression and a Heaviside step-gain function was analytically investigated in [33]. Numerical results for models with synaptic depression and smooth sigmoid gain functions were also reported in [33] and [31].

In the context of neuronal competition models we define *release* and *escape mechanisms* as follows: The two populations in the network oscillate in antiphase competing for the active state; for the dominant population of variable, say, u_1 , the net input $I - \beta u_2 - ga_1$ decreases as the slow negative feedback accumulates; on the contrary, for the suppressed population u_2 the feedback recovers (decays) so the net input $I - \beta u_1 - ga_2$ increases. However, since function S is highly nonlinear, equal changes in the net input $I - \beta u_j - ga_k$ of both populations can lead to drastically different changes in the corresponding effective response $S(I - \beta u_j - ga_k)$. This transformation has a direct influence on the variation of u_1 and u_2 . The switch in dominance is due either to a significant, more abrupt change (decrease) in the response to an input to the dominant population, or, on the contrary, to a significant change (increase) in the response to an input to the suppressed population. In the first case the dominant population loses control, its activity drops, and it no longer suppresses its competitor, which becomes active. We call this mechanism *release*. In the latter case, when the input-output function S of the suppressed population changes faster, this population regains control, its activity rises, and it forces its competitor into the inhibited state. We call this mechanism *escape*.

Intuitively, escape occurs for higher stimulus ranges than release. Therefore, we expect that an escape (release) mechanism underlies the dynamics in region II (region IV) in Figure 3F with decreasing (increasing) I - T curve. For large values of I the gain function for the dominant population is relatively constant and close to 1 while that for the suppressed population falls in the interval where it is steeper. For example, let us consider the fast plane (u_1, u_2) and assume that u_1 is ON and u_2 is OFF; then the dominance switching point is on the shallow part of the active population nullcline $u_1 = S(I - \beta u_2 - ga_1)$ and on steeper part of down population nullcline $u_2 = S(I - \beta u_1 - ga_2)$ (see the animation 70584_01.gif [3.7MB] in Appendix C). A larger variation in u_2 than in u_1 is expected, and that corresponds to the escape mechanism. For small values of I the gain function for the dominant population is steeper (the steeper part of active population nullcline $u_1 = S(I - \beta u_2 - ga_1)$), while the gain function for the suppressed population is relatively constant and close to 0 (the shallow part of the down population nullcline $u_2 = S(I - \beta u_1 - ga_2)$)—see the animation 70584_02.gif [3.8MB] in Appendix C. That is what we call release.

For sufficiently large inhibition β , at intermediate I the effective response to an input to both populations might end up being relatively constant: closer to 1 for the active population and closer to 0 for the down population. The switching does not take place anymore; instead a *winner-take-all* dynamics is obtained.

In the following we investigate analytically how the period of oscillations for system (2.1) depends on the input strength and show that the increasing (decreasing) branch of the I - T curve is associated with the release (escape) mechanism. Our analysis is done in two steps: first, in section 4.1, we consider the limiting case sigmoid function $S(x) = Heav(x - \theta)$ such that $S(x) = 0$ if $x < \theta$ and $S(x) = 1$ if $x > \theta$; the function does not obey the hypotheses in section 2, but it provides a useful example where escape, release, and winner-take-all dynamics are easily characterized. Then in section 4.2 we return to the case of smooth sigmoid function and describe the notions defined above in this more general context. We find a precise mathematical characterization for the minimum value of β and then for the corresponding input values, say,

I_w^* and I_w^{**} , where the winner-take-all regime appears. In the absence of a winner-take-all regime we provide a mathematical definition for the transition between escape and release.

4.1. A relevant example: The Heaviside step function

The choice of $S(x) = \text{Heav}(x-\theta)$ allows us to solve for completely the intervals of the stimulus strength I where oscillations and winner-take-all dynamics exist. For system (2.1) with a Heaviside step function, there are only four possible equilibrium points: $(1, 1, 1, 1)$, $(1, 0, 1, 0)$, $(0, 1, 0, 1)$, and $(0, 0, 0, 0)$. Here $(1, 1, 1, 1)$ and $(0, 0, 0, 0)$ correspond respectively to the simultaneously high and low activity states observed in numerical simulations in regions I and V of Figure 3F. Oscillations can occur only between the states $(u_1, u_2) = (1, 0)$ and $(u_1, u_2) = (0, 1)$ in which one population is dominant and the other one is suppressed. Let us now determine the necessary and sufficient conditions for the oscillations to exist. The idea used in our analysis is similar to that in [17] and [33].

In the fast plane, the nullclines of u_1 and u_2 consist in two constant plateaus of zero and unit value discontinuously connected at a “threshold” point $(I - (\theta + ga_1))/\beta$ and $(I - (\theta + ga_2))/\beta$, respectively (Figure 5A). During oscillation, due to the change in slow variables a_1 and a_2 these thresholds move along the vertical and horizontal axes. For example, assuming $u_1 = 1$, $u_2 = 0$, the slow equations become $\tau \dot{a}_1 = -a_1 + 1 > 0$ and $\tau \dot{a}_2 = -a_2 < 0$; thus the u_1 -nullcline moves down while the u_2 -nullcline moves to the right. If these nullclines slide enough and the thresholds cross either 0 (for the u_1 -nullcline) or 1 (for the u_2 -nullcline), i.e., either $a_{1J} = (I - \theta)/g$ or $a_{2J} = (I - (\theta + \beta))/g$ are reached, then the equilibrium point $(u_1, u_2) = (1, 0)$ disappears and the system will be attracted to $(u_1, u_2) = (0, 1)$. The switch takes place and the slow equations change to $\tau \dot{a}_1 = -a_1 < 0$, $\tau \dot{a}_2 = -a_2 + 1 > 0$, now pushing the nullclines in opposite directions. As we explain below, depending on which of the two *jumping values* a_{1J} or a_{2J} is reached first, a *release* or an *escape* mechanism will underlie the oscillation.

We note that for an oscillatory solution, $u_1 + u_2 = 1$ always, and so $\tau(\dot{a}_1 + \dot{a}_2) = 1 - (a_1 + a_2)$. Asymptotically, the slow dynamics will occur along the diagonal $a_1 + a_2 = 1$ of the unit square (Figure 5D or 5F). The positions the horizontal line $a_2 = (I - (\theta + \beta))/g$ and the vertical line $a_1 = (I - \theta)/g$ have relative to the unit square is important when the trajectory points to the lower-right corner; on the other hand, when the trajectory points to the upper-left corner, the position of vertical line $a_1 = (I - (\theta + \beta))/g$ and horizontal line $a_2 = (I - \theta)/g$ will matter. Therefore, in the slow plane (a_1, a_2) (see Figure 5B–5H) we are interested in the intersection of the unit square (grey) with the square defined by the possible jumping values $(I - (\theta + \beta))/g$ (blue) and $(I - \theta)/g$ (red). If the red line is reached, then the active cell ($u_j = 1$) becomes suddenly inactive ($u_j = 0$), allowing its competitor to go up. That is why we call this case a release mechanism; otherwise, if the blue line is reached first, then the suppressed cell becomes suddenly active, forcing its competitor to go down. That is the escape mechanism.

As parameter I decreases, the blue-red square slides down along the first diagonal, starts to intersect the grey unit square, and then leaves it (Figure 5B–5H). The way those two squares intersect determines the system’s dynamics, so we need to take into account the relative size of their sides: 1 and β/g .

Theorem 4.1 (five modes of behavior for large enough inhibition strength). *Let us assume that $\beta/g > 1$. The following five dynamical regimes exist for the neuronal competition model (2.1) with $S(x) = \text{Heav}(x - \theta)$.*

- i. *If $I \geq \theta + \beta + g/2$, then the system’s attractor is the simultaneously high activity state $u_1 = u_2 = 1$.*

- ii. If $\theta + \beta < I < \theta + \beta + g/2$, then the system oscillates between the states $(u_1, u_2) = (1, 0)$ and $(u_1, u_2) = (0, 1)$ due to an escape mechanism. The period of oscillations decreases with I and satisfies

$$T_{\text{escape}} = 2\tau \ln \left(\frac{g}{I - (\theta + \beta)} - 1 \right). \quad (4.1)$$

- iii. If $\theta + g \leq I \leq \theta + \beta$, then the system is in a winner-take-all regime with fast variables either $(1, 0)$ or $(0, 1)$ depending on the initial condition choice.
- iv. If $\theta + g/2 < I < \theta + g$, then the system oscillates between the states $(u_1, u_2) = (1, 0)$ and $(u_1, u_2) = (0, 1)$ due to a release mechanism. The period of oscillations increases with I and satisfies

$$T_{\text{release}} = 2\tau \ln \left(\frac{g}{\theta + g - I} - 1 \right). \quad (4.2)$$

- v. If $I \leq \theta + g/2$, then the system's attractor is the simultaneously low activity state $u_1 = u_2 = 0$.

Proof. Since $\beta/g > 1$, there are exactly seven relative positions of the blue-red square to the unit square that lead to conclusions (i) to (v).

- i. For $1 \leq (I - (\theta + \beta))/g$ (Figure 5B) both a_1, a_2 are smaller than $(I - (\theta + \beta))/g$, so $I - \beta u_i - g a_k \geq I - \beta - g \geq \theta$, and we always have $u_1 = u_2 = 1$.

If $1/2 \leq (I - (\theta + \beta))/g < 1 < (I - \theta)/g$ (Figure 5C), let us assume $u_1 = 1, u_2 = 0$, and $a_1 + a_2 = 1$ as initial values. The slow variable a_1 increases while a_2 decreases; in this case only a_2 can cross the horizontal blue line, producing the jump of u_2 from 0 to 1. However, just after the jump, in the equation of u_1 we have $I - \beta u_2 - g a_1 = I - \beta - g(1 - a_2) = 2(I - (\beta + \theta)) - g + \theta \geq \theta$, which keeps u_1 at its value 1. Therefore, the point will be attracted to the corner $(a_1, a_2) = (1, 1)$ and the oscillation dies.

- ii. For $0 < (I - (\theta + \beta))/g < 1/2 < 1 < (I - \theta)/g$ (Figure 5D), a_2 will first cross the blue line and induce a sudden change in u_2 . Then in the u_1 -equation we obtain $I - \beta u_2 - g a_1 = I - \beta - g(1 - a_2) = 2(I - (\beta + \theta)) - g + \theta < \theta$, which forces u_1 to take zero value. The fast system switches from $(1, 0)$ to $(0, 1)$ and the slow dynamics changes its direction of movement along the upper-left-lower-right diagonal of the unit square. The change $I - \beta u_1 - g a_2 = I - g a_2 \geq I - g \geq \theta$ does not affect the new value $u_2 = 1$; oscillation exists indeed and its projection on the slow plane is the segment defined by the intersection of the unit square's secondary diagonal with the two blue lines. When I decreases, the length of this segment increases, so it will take longer to go from one endpoint to the other. We expect the period T to increase as I decreases. Indeed, at the jumping point, the slow variable for the suppressed population takes the value $a_f := a_{2J} = (I - (\theta + \beta))/g$; however, just after the previous jump it was $a_i := 1 - a_{1J} = 1 - (I - (\theta + \beta))/g$. Therefore, from $\tau \dot{a}_2 = -a_2$ we compute the solution $a(t) = a_i e^{-t/\tau}, t \in (0, T/2)$. The period T of oscillation is $T = 2\tau \ln(a_i/a_f)$, i.e., exactly (4.1). Moreover, $dT/dI < 0$, so T decreases with I .

- iii. By choosing I such that $(I - (\theta + \beta))/g < 0 < 1 \leq (I - \theta)/g$, the unit square falls completely inside the blue-red square (Figure 5E). Starting at $u_1 = 1, u_2 = 0$ we have $I - \beta u_2 - g a_1 = I - g a_1 \geq I - g \geq \theta$ and $I - \beta u_1 - g a_2 = I - \beta - g a_2 \leq I - \beta < \theta$; the slow variables a_1 and a_2 continue to increase, respectively, decrease, approaching the

lower-right corner of the unit square, and a winner-take-all state is achieved. For $u_1 = 0, u_2 = 1$, the point (a_1, a_2) will be attracted to the upper-left corner.

- iv. Decreasing I even more, we enter the region $(I - (\theta + \beta))/g < 0 < 1/2 < (I - \theta)/g < 1$ (Figure 5F). Here the threshold is crossed at the red line and (when $u_1 = 1, u_2 = 0$) u_1 jumps from 1 to 0. In the u_2 -equation, the expression $I - \beta u_1 - g a_2$ becomes $I - g(1 - a_{1J}) = 2(I - \theta) - g + \theta \geq \theta$, which leads to $u_2 = 1$. That is the release mechanism. In the slow plane (a_1, a_2) the point changes its direction of movement; the oscillation occurs along the segment defined by the intersection of the unit square's secondary diagonal with the two red lines. The length of this segment decreases as I decreases; it takes less time to go from one endpoint to the other, so we expect the period T to decrease. Indeed, for the release mechanism, $a_f := a_{1J} = (I - \theta)/g$, with value just after the previous jump $a_i := 1 - a_{2J} = 1 - (I - \theta)/g$. The slow differential equation is now $\tau \dot{a}_1 = 1 - a_1$, that is, $a(t) = 1 - (1 - a_i)e^{-t/\tau}$, $t \in (0, T/2)$. The period T of oscillation satisfies $T = 2\tau \ln((1 - a_i)/(1 - a_f))$, or (4.2). Obviously $dT/dI > 0$.
- v. Oscillations cannot exist anymore for $(I - (\theta + \beta))/g < 0 < (I - \theta)/g < 1/2$ (Figure 5G). Say, that again, we have $u_1 = 1, u_2 = 0$: only a_1 can reach the threshold (red) line for u_1 to become inactive. However, just after the jump, in the u_2 -equation the net input $I - \beta u_1 - g a_2 = I - g(1 - a_{1J}) = 2(I - \theta) - g + \theta$ is still less than θ , and it keeps u_2 at zero. Both slow variables start to decrease approaching the corner $(a_1, a_2) = (0, 0)$. The oscillation dies, and the fast system has $(0, 0)$ as a single attractor. For even smaller values of input strength, $(I - (\theta + \beta))/g < (I - \theta)/g < 0$ (Figure 5H), it is true that $I - \beta u_i - g a_k \leq I < \theta$ and $u_1 = u_2 = 0$.

Remark 4.1. We note that in the escape regime, $T \rightarrow 0$ as $I \rightarrow \theta + \beta + g/2$ and $T \rightarrow \infty$ as $I \rightarrow \theta + \beta$. Similarly, in the release regime, $T \rightarrow 0$ as $I \rightarrow \theta + g/2$ and $T \rightarrow \infty$ as $I \rightarrow \theta + g$.

Case (iii) in Theorem 4.1 (case (E) in Figure 5) is not possible if the side of the blue-red square is smaller than the unit. Therefore, the winner-take-all dynamics is eliminated. On the other hand, the blue-red square can lie completely inside the unit square. Then we need to distinguish between two cases: the point moving along the secondary diagonal of the unit square may first reach the blue line (Figure 6A) or the red line (Figure 6B).

Theorem 4.2 (no winner-take-all regime for low inhibition strength). Let us assume that $\beta/g < 1$. Then the neuronal competition model (2.1) with $S(x) = \text{Heav}(x - \theta)$ exhibits only four dynamical regimes.

If $I \geq \theta + \beta + g/2$, then the system's attractor is the high activity state $u_1 = u_2 = 1$. Similarly, if $I \leq \theta + g/2$, the system's attractor is the low activity state $u_1 = u_2 = 0$.

For intermediate values of input strength, the system oscillates between the states $(u_1, u_2) = (1, 0)$ and $(u_1, u_2) = (0, 1)$. If $\theta + (\beta + g)/2 < I < \theta + \beta + g/2$, oscillations occur due to an escape mechanism; the period T decreases with I and satisfies (4.1). If $\theta + g/2 < I < \theta + (\beta + g)/2$, then a release mechanism underlies the oscillations and T increases with I according to (4.2).

Moreover, at $I_{Tmax} = \theta + (\beta + g)/2$ the system has maximum oscillation period

$$T_{max} = 2\tau \ln \left(\frac{1 + \beta/g}{1 - \beta/g} \right).$$

Proof. Let us assume again initial conditions $u_1 = 1, u_2 = 0$, and $a_1 + a_2 = 1$; therefore, a_1 increases and a_2 decreases. In order to first reach the blue line (Figure 6A), the inequality $1 - (I - (\theta + \beta))/g < (I - \theta)/g$, i.e., $I > I_{Tmax}$, must be true. When the blue line is reached, the down

variable u_2 switches from 0 to 1. If $(I - (\theta + \beta))/g < 1/2$, the net input for u_1 becomes $N_e := I - \beta u_2 - g a_1 = I - \beta - g(1 - a_2) = 2(I - \beta - \theta) - g + \theta < \theta$, so u_1 changes to 0 and oscillation occurs due to an escape mechanism. If $(I - (\theta + \beta))/g \geq 1/2$, then $N_e \geq \theta$ and u_1 remains 1; the fast system has $(1, 1)$ as an attractor. Similar arguments are used for the release mechanism; the condition for intersection with the red line (Figure 6B) is equivalent to the inequality $1 - (I - \theta)/g > (I - (\theta + \beta))/g$, i.e., $I < I_{Tmax}$. For both (4.1) and (4.2), $T \rightarrow T_{max}$ as $I \rightarrow \theta + (\beta + g)/2$. Also, $T_{escape} \rightarrow 0$ as $I \rightarrow \theta + \beta + g/2$ and $T_{release} \rightarrow 0$ as $I \rightarrow \theta + g/2$.

4.2. Global features of the competition model with smooth sigmoid gain function

Numerical simulations of system (2.1) with smooth gain function S indicate that the limit cycle born through the Hopf bifurcation as in section 3 takes a relaxation-oscillator form just beyond the bifurcation (Figure 3B and 3D). That is, because of the two time-scales involved in the system, variables u_1 and u_2 evolve much faster than a_1 and a_2 ($\tau \gg 1$). We use this observation to describe for (2.1) the relaxation-oscillator solution in the singular limit $1/\tau = 0$. In the plane (a_1, a_2) of slow variables we construct the curve of “jumping” points from the dominant to the suppressed state of each population, and back. This curve is the equivalent of the blue-red square from the case of Heaviside step function, and similarly it consists of two arcs associated with an escape and release mechanism, respectively. Then we give analytical conditions for the winner-take-all regime to exist.

4.2.1. The singular relaxation-oscillator solution—For large values of τ let us consider the slow time $s = \varepsilon t$ ($\varepsilon = 1/\tau$; $' = d/ds$) and rewrite system (2.1) as

$$\varepsilon u_1' = -u_1 + S(I - \beta u_2 - g a_1), \quad \varepsilon u_2' = -u_2 + S(I - \beta u_1 - g a_2), \quad a_1' = -a_1 + u_1, \quad a_2' = -a_2 + u_2.$$

In the singular perturbation limit $\varepsilon = 0$ any solution will belong to the slow manifold Σ defined by $-u_1 + S(I - \beta u_2 - g a_1) = 0$, $-u_2 + S(I - \beta u_1 - g a_2) = 0$ or, based on the inverse property of S ($S^{-1} = F$),

$$\Sigma = \left\{ (u_1, u_2, a_1, a_2) : u_1, u_2 \in (0, 1), a_1, a_2 \in \mathbf{R}, \quad \text{and} \quad u_2 = S(I - \beta u_1 - g a_2), a_1 = \frac{1}{g} [I - F(u_1) - \beta S(I - \beta u_1 - g a_2)] \right\}. \quad (4.3)$$

The surface Σ is multivalued and can be visualized by plotting a_1 as a function of u_1 and a_2 (Figure 7).

Then the slow dynamics is according to equations $a_1' = -a_1 + \tilde{u}_1(a_1, a_2)$, $a_2' = -a_2 + \tilde{u}_2(a_1, a_2)$, where $(\tilde{u}_1, \tilde{u}_2, a_1, a_2) \in \Sigma$. The “slow” nullclines are characterized by additional conditions: $a_1 = u_1$ for a_1 -nullcline (\mathcal{N}_1) and $a_2 = u_2$ for a_2 -nullcline (\mathcal{N}_2); geometrically these are two curves situated on the surface Σ and defined by

$$\begin{aligned} & \mathcal{N}_1(a_1'=0) \\ &= \left\{ (u_1, u_2, a_1, a_2) : u_1 = a_1, u_2 = S(I - \beta a_1 - g a_2(a_1)), a_2 = \frac{1}{g} \left[I - \beta a_1 - F\left(\frac{I - g a_1 - F(a_1)}{\beta}\right) \right] \text{ with } a_1 \in (\alpha_1, \alpha_2) \right\} \end{aligned} \tag{4.4}$$

and

$$\begin{aligned} & \mathcal{N}_2(a_2'=0) \\ &= \left\{ (u_1, u_2, a_1, a_2) : u_1 = S(I - \beta a_2 - g a_1(a_2)), u_2 = a_2, a_1 = \frac{1}{g} \left[I - \beta a_2 - F\left(\frac{I - g a_2 - F(a_2)}{\beta}\right) \right] \text{ with } a_2 \in (\alpha_1, \alpha_2) \right\}. \end{aligned} \tag{4.5}$$

Here $\alpha_1, \alpha_2 \in (0, 1)$ are the unique solutions of the equations $F(\alpha_1) + g\alpha_1 = I - \beta$ and $F(\alpha_2) + g\alpha_2 = I$, respectively.

The equilibrium points are at the nullclines' intersection, which means $a_1 = u_1$ and $a_2 = u_2$ simultaneously on Σ . They are characterized by the conditions

$$\mathcal{N}_1 \cap \mathcal{N}_2 : u_1 = a_1, u_2 = a_2, F(a_1) + g a_1 + \beta a_2 = F(a_2) + g a_2 + \beta a_1 = I. \tag{4.6}$$

We recall from section 3 that if $\beta > \left(1 + \frac{1}{\tau}\right) / S'(\theta)$ (which in the limit case $\varepsilon = 0$ corresponds to $\beta > 1/S'(\theta)$), there exist two values of input parameter $I_{hb}^* < I_{hb}^{**}$ such that the system has a unique stable equilibrium point for $I \in (-\infty, I_{hb}^*) \cup (I_{hb}^{**}, \infty)$. This equilibrium point takes the form $\mathbf{e}_I = (u_I, u_I, u_I, u_I)$ with $u_I \in (0, 1)$, $F(u_I) + (\beta + g)u_I = I$, and it becomes unstable at I_{hb}^* and I_{hb}^{**} , a stable limit cycle appears for $I > I_{hb}^*$ and $I < I_{hb}^{**}$. The critical parameter values are defined by $I_{hb}^* = F(u_{hb}^*) + (\beta + g)u_{hb}^*$ and $I_{hb}^{**} = F(u_{hb}^{**}) + (\beta + g)u_{hb}^{**}$ with u_{hb}^*, u_{hb}^{**} according to (3.5). Again, in the limit case $\varepsilon = 0$, condition (3.5) becomes

$$F'(u_{hb}^*) = F'(u_{hb}^{**}) = \beta, \tag{4.7}$$

and obviously we have $F'(u_I) < \beta$ for each $I \in (I_{hb}^*, I_{hb}^{**})$.

Moreover, if $\beta - g > 1/S'(\theta)$, two additional equilibrium points occur for $I > I_{pf}^*$ and $I < I_{pf}^{**}$ through a pitchfork bifurcation. However, at least in the neighborhood of I_{pf}^* or I_{pf}^{**} , these

equilibrium points are unstable. Their coordinates (u_{1p}, u_{2p}) satisfy (4.6), so either $u_{1p} < u_I < u_{2p}$ or $u_{1p} > u_I > u_{2p}$. In addition, they are close to u_I for all I sufficiently close to I_{pf}^* or I_{pf}^{**} ; in conclusion, at least in a small region, $F'(u_{1p}) < \beta$ and $F'(u_{2p}) < \beta$.

In Figure 7 we plotted the projection on the three-dimensional space (u_1, a_1, a_2) of the slow manifold Σ and the nullclines \mathcal{N}_1 and \mathcal{N}_2 (\mathcal{N}_1 is colored in magenta and \mathcal{N}_2 is colored in black; because Σ is defined over the full range $-\infty$ to ∞ with respect to a_1 and a_2 , we plot only part of it). All plots are done for S as in (2.2), $\beta = 1.1$, $g = 0.5$, $r = 10$, $\theta = 0.2$, and two values of input strength, $I = 1.5$ (Figure 7A–C) and $I = 1$ (Figure 7D–F). For these values of parameters we have $I_{pf}^* = 0.4064$ and $I_{pf}^{**} = 1.5936$, so at both $I = 1.5$ and $I = 1$ the system has three equilibrium points; nullclines intersect three times and the middle intersection point is exactly \mathbf{e}_I . We note that all equilibrium points are unstable at $I = 1.5$ while two of them become stable at $I = 1$ (see also Figure 3G).

On the surface Σ we have $\frac{\partial u_1}{\partial a_1} = g / \left[\beta^2 S'(I - \beta u_1 - g a_2) - F'(u_1) \right]$ and $\frac{\partial u_1}{\partial a_2} = -\beta g / \left[\beta^2 - F'(u_1) / S'(I - \beta u_1 - g a_2) \right]$, i.e.,

$$\frac{\partial u_1}{\partial a_1} = \frac{g F'(u_2)}{\beta^2 - F'(u_1) F'(u_2)} \quad \text{and} \quad \frac{\partial u_1}{\partial a_2} = -\frac{\beta g}{\beta^2 - F'(u_1) F'(u_2)}.$$

For an initial condition (u_1, u_2, a_1, a_2) with u_1 sufficiently large (close to 1) we have $\frac{\partial u_1}{\partial a_1} < 0$ and $\frac{\partial u_1}{\partial a_2} > 0$; therefore, a simultaneous increase in a_1 and decrease in a_2 lead to a decrease in

u_1 . Similarly, for a choice of u_1 sufficiently low (close to 0), $\frac{\partial u_1}{\partial a_1} < 0$, $\frac{\partial u_1}{\partial a_2} > 0$, and a simultaneous decrease in a_1 and increase in a_2 lead to an increase in u_1 . On the other hand, the limit cycle

exists for some $I \in (I_{hb}^*, I_{hb}^{**})$. Since here $\mathbf{e}_I \in \Sigma$ with $F'(u_I) < \beta$, we have $\frac{\partial u_1}{\partial a_1} > 0$ and $\frac{\partial u_1}{\partial a_2} < 0$ in a neighborhood of this equilibrium point; the behavior of u_1 with respect to a_1 and a_2 is opposite that previously described.

Therefore, relative to the plane (u_1, a_1) the surface Σ has a cubic-like shape: its left and right branches decrease with u_1 while the middle branch increases. The curve of lower ($u_1 < u_2$) and upper ($u_1 > u_2$) knees on Σ is defined by $F'(u_1)F'(u_2) = \beta^2$ (blue-red curve in Figure 7C and 7F). As we show in the following, when the trajectory on surface Σ reaches the curve of knees on its upper side, the point will jump from the right branch of Σ to its left branch. Similarly, when it reaches the lower side of the curve of knees, the point will jump from the left to the right branch of Σ . In the plane of fast variables (u_1, u_2) the curve of knees corresponds to a saddle-node bifurcation (a node approaching a saddle then merging with it and disappearing—see the animations 70584_01.gif [3.7MB] and 70584_02.gif [3.8MB] in Appendix C). For this reason we also call it the *curve of saddle-nodes (SN)* or the *curve of jumping points*. It is defined by the equations

$$SN: F'(u_{1j}) F'(u_{2j}) = \beta^2, a_{1j} = \frac{1}{g} [I - F(u_{1j}) - \beta u_{2j}], a_{2j} = \frac{1}{g} [I - F(u_{2j}) - \beta u_{1j}]. \tag{4.8}$$

We do not prove here the existence of the relaxation-oscillator singular solution. We aim only to provide the reader with the intuition for how oscillations occur in the competition model (2.1) if a smooth sigmoid is taken as a gain function. Thus, if the oscillations exist and, for example, u_1 is dominant and u_2 is suppressed ($u_1 > u_2$), we have $-a_1 + u_1 > 0$, $-a_2 + u_2 < 0$, so a_1 increases and a_2 decreases. They push u_1 down and the point moves on the trajectory

until it reaches \mathcal{SN} at an upper knee U of coordinates (u_{1J}, u_{2J}) ; here the derivatives $\frac{\partial u_1}{\partial a_1}$ and $\frac{\partial u_1}{\partial a_2}$ become infinite, so u_1 jumps from the upper to the lower branch of Σ (Figure 8A–8B). On the lower branch ($u_1 < u_2$) we have $-a_1 + u_1 < 0$ and $-a_2 + u_2 > 0$, so u_1 increases and the point will move due to the decrease of a_1 and increase of a_2 until it touches \mathcal{SN} at L . At L the point jumps up to the right branch of Σ . The projection of the limit cycle on the slow plane (a_1, a_2) is a closed curve that touches the projection of \mathcal{SN} at two points (a_{1J}, a_{2J}) and (a_{2J}, a_{1J}) symmetric to the line $a_1 = a_2$ (Figures 8C and 9B).

4.2.2. Release, escape, and winner-take-all in the competition model with smooth sigmoid gain function—Analogous to our analysis in section 4.1 we consider in the following the projection of the curve of jumping points \mathcal{SN} on the slow plane (a_1, a_2) . As mentioned above, if the up-to-down jump takes place at (a_{1J}, a_{2J}) , then the down-to-up jump is at (a_{2J}, a_{1J}) ; so the projection is a closed curve symmetric to the diagonal $a_1 = a_2$.

We consider in (a_1, a_2) the curve Γ_0 of equations

$$A_1 = -\frac{1}{g} [F(u_{1J}) + \beta u_{2J}], \quad A_2 = -\frac{1}{g} [F(u_{2J}) + \beta u_{1J}]$$

with $F'(u_{1J})F'(u_{2J}) = \beta^2$. Then from (4.8) we have

$$a_{1J} = A_1 + \frac{I}{g}, \quad a_{2J} = A_2 + \frac{I}{g}.$$

For a given I , the projection of \mathcal{SN} on the slow plane (say, $\Gamma = \Gamma_I$) is exactly the translation of Γ_0 with quantity $(I/g, I/g)$ along the first bisector. Obviously as I decreases, the curve Γ moves down on the upper-right–lower-left direction (Figure 9B). That is similar to the movement of the blue-red square for the case of the Heaviside step function in section 4.1 (Figure 5).

Let us consider now an oscillatory solution that exists for some $I \in (I_{hb}^*, I_{hb}^{**})$. If population 1 is dominant ($u_1 > u_2$), then $-a_1 + u_1 > 0$ and $-a_2 + u_2 < 0$ imply $u_1 - u_2 > a_1 - a_2$. On the other hand, since the trajectory is on Σ , we also have $a_1 = [I - F(u_1) - \beta u_2]/g$, $a_2 = [I - F(u_2) - \beta u_1]/g$, and thus $a_1 - a_2 = [\beta(u_1 - u_2) - (F(u_1) - F(u_2))]/g$. At the jumping point a_1 reaches its maximum and a_2 its minimum, so $0 < a_{1J} - a_{2J} < u_{1J} - u_{2J}$ can be written as

$$0 < W(u_{1J}) = \frac{1}{g} \left(\beta - \frac{F(u_{1J}) - F(u_{2J})}{u_{1J} - u_{2J}} \right) < 1. \tag{4.9}$$

The point (u_{1J}, u_{2J}) , $u_{1J} > u_{2J}$, satisfies $F'(u_{1J})F'(u_{2J}) = \beta^2$ and describes the part of \mathcal{SN} that corresponds to the upper knees. Let $u_{m\beta}, u_{M\beta} \in (0, 1)$ be the values defined by $u_{m\beta} < u_{hb}^* < u_0 < u_{hb}^{**} < u_{M\beta}$, $F'(u_{m\beta}) = F'(u_{M\beta}) = \beta^2/F'(u_0) = \beta^2 S'(\theta)$ (see the shape of F' in Figure 2C). Then the upper branch of \mathcal{SN} results by gluing together three arcs on which (1) u_{1J}

increases between u_{hb}^{**} and $u_{M\beta}$ (so u_{2J} decreases from u_{hb}^{**} to u_0); (2) u_{1J} decreases from $u_{M\beta}$ to u_0 (and u_{2J} decrease from u_0 to $u_{m\beta}$); (3) u_{1J} continues to decrease from u_0 to u_{hb}^* (however, u_{2J} increases now between $u_{m\beta}$ and u_{hb}^*).

We can plot the expression $W(u_{1J})$ from (4.9) for $u_{1J} \in [u_{hb}^{**}, u_{M\beta}]$ and $u_{1J} \in [u_{hb}^*, u_{M\beta}]$ with the corresponding $u_{2J} = u_2(u_{1J})$ and check if the graph is below the horizontal line $W = 1$ (Figure 9A). If for all combinations (u_{1J}, u_{2J}) we have $W < 1$, then the winner-take-all regime does not exist in the interval (I_{hb}^*, I_{hb}^{**}) . Otherwise, for (u_{1J}, u_{2J}) where $W = 1$ we can compute the values of I where winner-take-all occurs (see below).

Remark 4.2. Let us observe that $W(u_{1J}) = [\beta - F'(\xi)]/g$ for some intermediate ξ between u_{2J} and u_{1J} . At $u_{1J} = u_{2J} = u_{hb}^{**}$ or $u_{1J} = u_{2J} = u_{hb}^*$ (that represents exactly the equilibrium point e_I at $I = I_{hb}^{**}$ and I_{hb}^* respectively) we have $F'(\xi) = \beta$; therefore, we can extend by continuity the function $W|_{[u_{hb}^{**}, u_{M\beta}]}$ at $u_{1J} = u_{hb}^{**}$ and the function $W|_{[u_{hb}^*, u_{M\beta}]}$ at $u_{1J} = u_{hb}^*$ by taking $W = 0$ at these edges.

For gain function S as in (2.2) and different values of β we plotted the curve W ; the curve W always has a maximum value W_{max} for some $u_{1J}^{W_{max}} \in (u_0, u_{M\beta})$ with $u_2 = u_2(u_{1J}) \in (u_{m\beta}, u_0)$. Here $||u_{2J}||u_{1J} = -[F''(u_2)F''(u_1)]/[F'(u_1)F''(u_2)] > 0$. W measures the relative distance between the values of slow variables against that between fast variables. Based on this observation we color \mathcal{SN} , and obviously Γ , in blue for (u_{1J}, u_{2J}) starting at $(u_{hb}^{**}, u_{hb}^{**})$ and varying until it reaches $(u_{1J}^{W_{max}}, u_{2J}^{W_{max}})$ and in red for (u_{1J}, u_{2J}) between $(u_{1J}^{W_{max}}, u_{2J}^{W_{max}})$ and (u_{hb}^*, u_{hb}^*) (Figures 7C, 9B). The first corresponds to the right branch of W from $W = 0$ to W_{max} , and the latter corresponds to the left branch of W from W_{max} to 0.

Well inside the interval that defines the blue part of Γ (that is, not too close to the value $u_{1J}^{W_{max}}$ that gives the maximum W) we have either $u_0 < u_{2J} < u_{hb}^{**} < u_{1J}$ or $u_{hb}^* < u_{2J} < u_0 < u_{hb}^{**} < u_{1J}$; so $F'(u_{2J}) < \beta < F'(u_{1J})$. However, we recall that $F'(u_{2J}) = 1/S'(I - \beta u_{2J} - ga_{2J})$ and $F'(u_{1J}) = 1/S'(I - \beta u_{1J} - ga_{1J})$. That means that the gain function S has at the jump a bigger slope at $I - \beta u_{1J} - ga_1$, the net input to the suppressed population, than at $I - \beta u_{2J} - ga_2$, the net input to the dominant population; in other words, the gain to the suppressed population falls in the range of steeper S . According to the definitions introduced at the beginning of section 4, this case corresponds to an *escape* type of dynamics.

On the red part of Γ there is an opposite behavior: at least away from the edge $u_{1J}^{W_{max}}$ we have either $u_{2J} < u_{hb}^* < u_0 < u_{1J} < u_{hb}^{**}$ or $u_{2J} < u_{hb}^* < u_{1J} < u_0 < u_{hb}^{**}$. That is, $F'(u_{2J}) = 1/S'(I - \beta u_{1J} - ga_{2J}) > \beta > F'(u_{1J}) = 1/S'(I - \beta u_{2J} - ga_{1J})$. At the jump the gain $S'(I - \beta u_2 - ga_1)$ to the dominant population falls in the range of steeper S than that to the suppressed population. We called this a *release* mechanism.

In fact, the values $u_{2J}^{W_{max}}$ and $u_{1J}^{W_{max}}$ with $u_{2J}^{W_{max}} < u_0 < u_{1J}^{W_{max}}$ (and not u_{hb}^* and u_{hb}^{**}) determine what we generically call the “steeper” part of S . For the particular case of gain function symmetric to its inflection point (θ, u_0) , i.e., for S such that $S(\theta + x) + S(\theta - x) = 1$ it can be shown that indeed $u_{2J}^{W_{max}} = u_{hb}^*$ and $u_{1J}^{W_{max}} = u_{hb}^{**}$ (for example, S as in (2.2); see Remark 4.3). However, in other cases that is not true anymore; then it is more difficult to interpret the terms escape and release for u_{1J} close to $u_{1J}^{W_{max}}$, the passage point from one dynamical regime to another.

Occurrence of the winner-take-all regime: We can determine now the minimum value of β , say, β_{wta} , where the winner-take-all regime occurs in system (2.1). Moreover, for a given $\beta > \beta_{wta}$ we find the corresponding values of I that delineate this regime.

We note that if $I \in (I_{hb}^*, I_{pf}^*) \cup [I_{pf}^{**}, I_{hb}^{**})$, then system (2.1) has a unique equilibrium point and it belongs to the middle branch of Σ ($F'(u_I) < \beta$).

For $I > I_{pf}^*$ or $I < I_{pf}^{**}$ sufficiently close to the pitchfork bifurcation point, system (2.1) has three equilibria and all are situated again on the middle branch of Σ , inside \mathcal{SN} , the curve of lower and upper knees (Figure 7A and 7C). That is because $F'(u_{1p}) < \beta$ and $F'(u_{2p}) < \beta$, so $F'(u_{1p})F'(u_{2p}) < \beta^2$. A trajectory that starts on either the upper or the lower branch of Σ cannot approach an equilibrium point since it will first reach \mathcal{SN} , and so the system oscillates. However, for intermediate values of I between I_{pf}^* and I_{pf}^{**} , two of the equilibrium points may move on the lateral branches of Σ and become stable ($F'(u_{1p})F'(u_{2p}) > \beta^2$; see Figure 7D and 7F). That is the case where the winner-take-all regime occurs. We should point out that the equilibrium $e_I = (u_I, u_I, u_I, u_I)$ always remains unstable for $I \in (I_{pf}^*, I_{pf}^{**}) \subset (I_{hb}^*, I_{hb}^{**})$. The boundary between oscillatory and winner-take-all dynamics is obtained when the equilibrium points (u_{1p}, u_{2p}) belong to \mathcal{SN} , that is, when on \mathcal{SN} both $a_1 = u_1$ and $a_2 = u_2$ are true. We find in the following the values of I where winner-take-all appears.

The values of I , say, I_w , that delineate the winner-take-all regime are defined by

$$\begin{aligned} F'(u_{1J})F'(u_{2J}) &= \beta^2, \\ \frac{1}{g} \left(\beta - \frac{F(u_{1J}) - F(u_{2J})}{u_{1J} - u_{2J}} \right) &= 1, \\ I_w &= F(u_{1J}) + gu_{1J} + \beta u_{2J} \quad [= F(u_{2J}) + gu_{2J} + \beta u_{1J}]. \end{aligned} \tag{4.10}$$

The left-hand side of the second equation in (4.10) is in fact $W(u_{1J})$. Since the curve W always has a maximum value W_{max} for some $u_{1J}^{W_{max}} \in (u_0, u_{M\beta})$, the line $W = 1$ can be either above the maximum or below it. If $W_{max} < 1$ (Figure 9A, $\beta = 0.75$), then there is no winner-take-all regime. If $W_{max} > 1$ (Figure 9A, $\beta = 1.1$), then there exist two values for u_{1J} where the curve W intersects the horizontal line $W = 1$.

The critical (minimum) value β_{wta} where the winner-take-all regime appears in system (2.1) results from the case of $W_{max} = 1$; i.e., it satisfies the conditions $W(u_{1J}) = 1$ and $W'(u_{1J}) = 0$. Thus the minimum value β_{wta} that introduces winner-take-all dynamics in system (2.1) is defined by

$$\begin{aligned} F'(u_{1J})F'(u_{2J}) &= \beta^2, \quad u_{1J} \neq u_{2J}, \\ (F(u_{1J}) - F(u_{2J})) \left[F'(u_{1J})F''(u_{2J}) + F'(u_{2J})F''(u_{1J}) \right] &= (u_{1J} - u_{2J}) \left[F'(u_{1J})^2 F''(u_{2J}) + F'(u_{2J})^2 F''(u_{1J}) \right], \\ \beta_{wta} &= g + \frac{F(u_{1J}) - F(u_{2J})}{u_{1J} - u_{2J}}. \end{aligned} \tag{4.11}$$

Remark 4.3. We note that due to its particular form (2.2), S is symmetric about the point (θ, u_0) with $u_0 = 0.5$. The graph of F' is symmetric to the vertical line $u = 0.5$, i.e., $F'(1 - u) = F'(u)$ for all $u \in (0, 1)$, and so $F''(1 - u) = F''(u)$. In this particular case we have

$F'(u_{hb}^*) = F'(u_{hb}^{**}) = \beta$, so $u_{hb}^* = 1 - u_{hb}^{**}$ and $F''(u_{hb}^*) = -F''(u_{hb}^{**})$. According to (4.11) the maximum value W_{max} is obtained exactly at $u_{1J} = u_{hb}^{**}$, $u_{2J} = u_{hb}^*$.

For gain function S as in (2.2) and different values of β we plotted the curve W and determined the interval $[I_w^*, I_w^{**}]$ where winner-take-all occurs. For example, choosing $r = 10$, $\theta = 0.2$, $g = 0.5$, and $\beta = 1.1$, we have $W_{max} = 1.1046$ and $I_w^* = 0.697$ (computed at $u_{1J} = 0.7158$, $u_{2J} = 0.0424$) and $I_w^{**} = 1.303$ (computed at $u_{1J} = 0.9576$, $u_{2J} = 0.2842$). The minimum value of β for the winner-take-all regime is $\beta_{wta} = 1.0387$. As expected from our analysis in section 3.3, the value of β that guarantees existence of multiple equilibria in system (2.2), i.e., $\beta_{pf} = g + 1/S'(\theta) = 0.9$, is smaller than β_{wta} .

For the same choice of parameters as above ($\beta = 1.1$, $g = 0.5$, and S as in (2.2) with $r = 10$, $\theta = 0.2$), we plot the projection of the limit cycle and the curve of saddle-nodes on the slow plane (a_1, a_2) for different values of parameter I . Figure 10A gives the bifurcation diagram of activity u_1 versus input strength I for $\tau = 100$. In the rest of the panels we choose $\tau = 5000$ to mimic the singular limit cycle solution with jumping points exactly on the curve of saddle-nodes (for smaller τ , e.g., $\tau = 100$, the jumping points do not belong to the curve of saddle-nodes but fall close to it). In this case we have

$$I_{hb}^* = 0.1434, I_{pf}^* = 0.4064, I_w^* = 0.697, I_w^{**} = 1.303, I_{pf}^{**} = 1.5936, I_{hb}^{**} = 1.8566.$$

At larger values of I ($I = 1.7$ and $I = 1.5$) oscillation is due to an escape mechanism (Figure 10B–C); at an intermediate value $I = 1$ the system is in the winner-take-all regime (Figure 10D); at smaller values of I ($I = 0.5$ and $I = 0.3$) oscillation is due to a release mechanism (Figure 10E–F). Besides the limit cycle other important trajectories are the equilibrium points. There are three unstable equilibria for $I = 1.5$ and $I = 0.5$ but only one equilibrium point at $I = 1.7$ and $I = 0.3$. At $I = 1$ two out of three equilibria are stable.

Remark 4.4. Equations (4.11) and (4.10), used to determine the critical β where the winner-take-all regime exists in system (2.1) and then, for $\beta > \beta_{wta}$, to estimate I_w^* and I_w^{**} , prove to be reliable. The estimations obtained by this method are in excellent agreement with the results found in system (2.1)'s numerical simulations for both symmetric and asymmetric gain functions. The latter case is discussed in section 5.

5. Neuronal competition models that favor the escape (or release) dynamical regime

As seen in section 4.1, the dynamical scheme of T versus I is symmetric to $I = \theta + \frac{\beta + g}{2}$ for S , the Heaviside step function. When the winner-take-all regime exists, its corresponding I -input

interval is equally split around the value $\theta + \frac{\beta + g}{2}$, that is, $\theta + g \leq I \leq \theta + \beta$ as in Theorem 4.1. Moreover, an equal input range is found for both release and escape mechanisms:

$$\theta + \frac{g}{2} < I < \theta + g \text{ and } \theta + \beta < I < \theta + \beta + \frac{g}{2} \text{ as in Theorem 4.1, or } \theta + \frac{g}{2} < I < \theta + \frac{\beta + g}{2} \text{ and}$$

$\theta + \frac{\beta + g}{2} < I < \theta + \beta + \frac{g}{2}$ as in Theorem 4.2. Therefore, it seems reasonable to ask to what extent the symmetry of the I - T dynamical scheme about a specific value I^* relates to the geometry of S and, more generally, to the form of the equations in (2.1). We address this question in the following and find a heuristic method to reduce one of the two ranges of escape and release mechanisms while still maintaining the other one.

First let us note that we obtain a result similar to that in section 4.1 for any smooth sigmoid S as long as it is symmetric about its *threshold*. The threshold (say, th) is defined as the value where the gain function reaches its middle point: for S taking values between 0 and 1, it is S

$(th) = 0.5$. The terminology comes from the fact that if a net input to one population is below the threshold ($x < th$), then it determines a weak effective response ($S(x) < 1/2$); at equilibrium that would correspond to an inactive state. On the other hand, a net input above the threshold ($x > th$) determines a strong effective response ($S(x) > 1/2$) which, at equilibrium, corresponds to an active state. The *symmetry condition* of S with respect to the threshold is described mathematically by the equality $S(th + x) + S(th - x) = 1$ for any real x or, equivalently, $S(x) + S(2th - x) = 1$. The gain function defined by (2.2) is such an example: in this case the threshold is exactly the inflection point θ ($S''(\theta) = 0$; $S(\theta) = 0.5$).

Theorem 5.1. *If the gain function S satisfies $S(\theta + x) + S(\theta - x) = 1$, then system (2.1) with input I^* is diffeomorphic equivalent to system (2.1) with input $I = 2\theta + \beta + g - I^*$.*

Proof. Due to the symmetry of S , equation $\dot{\tilde{u}}_1 = -\tilde{u}_1 + S(I^* - \beta\tilde{u}_2 - g\tilde{a}_1)$ with the change $u_1 = 1 - \tilde{u}_1$, $u_2 = 1 - \tilde{u}_2$, $a_1 = 1 - \tilde{a}_1$, $a_2 = 1 - \tilde{a}_2$ becomes $\dot{u}_1 = -u_1 + 1 - S(I^* - \beta(1 - u_2) - g(1 - a_1)) = -u_1 + S((2\theta + \beta + g - I^*) - \beta u_2 - g a_1)$; on the other hand, equation $\tau \dot{\tilde{a}}_1 = -\tilde{a}_1 + \tilde{u}_1$ becomes $\tau \dot{a}_1 = -a_1 + u_1$. Therefore, system (2.1) with input I^* is diffeomorphic equivalent to system (2.1) with input $(2\theta + \beta + g - I^*)$.

Remark 5.1. *Theorem 5.1 implies that system (2.1) has the same type of solutions for any two values of input strength I_1 and I_1^* such that $\frac{1}{2}(I_1 + I_1^*) = \theta + \frac{\beta + g}{2}$. Moreover, if at I_1 and I_1^* an oscillatory solution of period T_1 and T_1^* exists, then, due to the diffeomorphism, $T_1 = T_1^*$.*

Obviously, if $T_1 < T_2$ for $I_1 < I_2 < \theta + \frac{\beta + g}{2}$, then $T_1^ < T_2^*$ for the corresponding values $I_1^* > I_2^* > \theta + \frac{\beta + g}{2}$. Therefore, for symmetric S to its inflection point (threshold in this case), the intervals of I for regions II and IV (see Figure 3F or H) have the same length and are symmetric to the line $I = \theta + \frac{\beta + g}{2}$.*

In order to explore the effect the asymmetry of S has on the bifurcation diagram, we consider S to be

$$S(x) = \begin{cases} 2u_0 / \left(1 + e^{-\frac{r}{2u_0}(x-\theta)}\right), & x \leq \theta, \\ 1 - 2(1 - u_0) / \left(1 + e^{-\frac{r}{2(1-u_0)}(\theta-x)}\right), & x > \theta, \end{cases} \tag{5.1}$$

with $u_0 \in (0, 1)$.

Therefore the inflection point θ and the threshold th satisfy $S(\theta) = u_0$ and $th > \theta$ if $u_0 < 1/2$, respectively, $th < \theta$ if $u_0 > 1/2$.

The graphs of S as in (5.1) and their corresponding F^* (where $F = S^{-1}$) are drawn in Figure 11A–B with parameter values $r = 10$, $\theta = 0.2$, and $u_0 = 0.1, 0.5, 0.9$. Then the I - T bifurcation diagram for the competition model (2.1) is constructed at $\beta = 0.75$ (Figure 11C). Numerical results show that the symmetry of this bifurcation diagram is indeed a direct consequence of the symmetry of S to its threshold. Such is the case $u_0 = 0.5$. For other choices of u_0 one of the two regions that correspond to the increasing and decreasing I - T branch is favored (it is wider)—the former when $u_0 > 1/2$ and the latter when $u_0 < 1/2$.

Recall from section 4 the definition (4.8) for the curve SN of jumping points (with its projection Γ on the plane of slow variables (a_1, a_2)) and the definition (4.9) for W that characterizes escape, release, and winner-take-all regimes. The shape of W changes dramatically with u_0 (Figure 11D, $\beta = 0.75$) but not at all with β . However, for any fixed u_0 the curve W always has a unique maximum point; this maximum moves down as β decreases.

The asymmetry of S leads to an asymmetry of the curve Γ : for $u_0 < 1/2$ we have $u_0 < u_{1J}^{W_{max}} < u_{hb}^{**}, u_{2J}^{W_{max}} < u_{hb}^*$, and the curves SN and Γ have a longer blue part than red part; the escape mechanism is favored (Figure 11E, $u_0 = 0.1$). On the contrary, for $u_0 > 1/2$ the release mechanism is favored since the red part of Γ is longer: $u_{1J}^{W_{max}} > u_{hb}^{**}$ and $u_{hb}^* < u_{2J}^{W_{max}} < u_0$ (Figure 11F, $u_0 = 0.9$). We can understand this specific behavior by looking at the network populations' dynamics about the threshold: in case of $u_0 < 1/2$ the maximum gain to each population is reached for some net input *below* the threshold ($S'(\theta) = \max S'$ with $S(\theta) = u_0$, so $\theta < th$); then about the threshold th the gain S' has a decreasing trend. Consequently, there is a wider range for inputs where the inactive population has a significant gain compared to the active population, and so the escape mechanism is favored (the suppressed population regains control on its own, thus becoming active). On the other hand, if $u_0 > 1/2$, the maximum gain to the network's populations is reached for some net input *above* the threshold ($\theta > th$) and the gain has an increasing trend in the vicinity of th . Therefore, the release mechanism is indeed much more easily obtained.

Remark 5.2. *The function S defined by (5.1) does not entirely satisfy the hypotheses introduced in section 2. In this case $F'''(u_0)$ does not exist anymore at $u_0 \neq 1/2$ even if we still have F as $C^2(0, 1)$ and $C^\infty((0, 1) \setminus \{u_0\})$. Nevertheless this property does not affect our analytical results (e.g., the expansion we used in section 3 to prove the existence of stable oscillatory solutions still makes sense since it is done locally about some point u^* different than u_0). Consequently, all the results found for system (2.1) in previous sections remain valid.*

5.1. A competition model that favors escape

In [31] we investigated four distinct neuronal competition models: a model by Wilson [37], one by Laing and Chow (the LC-model [17]), and two other variations of the LC-model that we called depression-LC and adaptation-LC. The latter is exactly the system (2.1) with symmetric sigmoid function. Besides the models' commonalities we also noticed some differences: in some cases the bifurcation diagrams show a preference of the system to the escape mechanism (the region of I that corresponds to the decreasing I - T branch is wider; see Figures 3 and 4 in [31]). Moreover, for sufficiently low inhibition in Wilson's and the depression-LC models the increasing (release-related) branch can disappear completely. Based on the results obtained in the present paper, we can explain those numerical observations.

Let us take, for example, Wilson's model for binocular rivalry [37,31]. Since the time-scale for inhibition is much shorter than the time-scale for the (excitatory) firing rate, we can assume that the inhibitory population tracks the excitatory population almost instantaneously. Thus Wilson's model becomes equivalent to a system of the form

$$\begin{aligned} \dot{u}_1 &= -u_1 + \frac{\gamma(I - \beta u_2)_+^2}{(\theta + a_1)^2 + (I - \beta u_2)_+^2}, \\ \dot{u}_2 &= -u_2 + \frac{\gamma(I - \beta u_1)_+^2}{(\theta + a_2)^2 + (I - \beta u_1)_+^2}, \\ \tau \dot{a}_1 &= -a_1 + g u_1, \\ \tau \dot{a}_2 &= -a_2 + g u_2, \end{aligned} \tag{5.2}$$

where γ is a positive constant and $[x]_+$ is defined as $[x]_+ = 0$ if $x < 0$ and $[x]_+ = x$ if $x \geq 0$. As in (2.1), parameters β and g represent here the strength of the inhibition and adaptation; I is the external input strength. We see that in the differential equations for u_j the nonlinearity is introduced through a function

$$\tilde{S}(x; \Theta) = \frac{\gamma [x]_+^2}{\Theta^2 + [x]_+^2},$$

that is, $\dot{u}_1 = -u_1 + \tilde{S}(I - \beta u_2; \theta + a_1)$ and $\dot{u}_2 = -u_2 + \tilde{S}(I - \beta u_1; \theta + a_2)$. We note that \tilde{S} is asymptotic to γ as $x \rightarrow \infty$ and satisfies $\tilde{S} = 0$ for $x \leq 0$ and $\tilde{S}(\Theta; \Theta) = \gamma/2$, which means Θ is the threshold. To compare system (5.2)'s dynamics with that of (2.1), we will assume without loss of generality that $\gamma = 1$.

By the change of variables $w_1 = \beta u_1 - I$, $w_2 = \beta u_2 - I$, $A_1 = \beta a_1/g - I$, $A_2 = \beta a_2/g - I$, the system (5.2) is diffeomorphic equivalent to

$$\begin{aligned} \dot{w}_1 &= -w_1 + \beta \tilde{S}(-w_2; \theta_1) - I, \\ \dot{w}_2 &= -w_2 + \beta \tilde{S}(-w_1; \theta_2) - I, \\ \tau \dot{A}_1 &= -A_1 + w_1, \\ \tau \dot{A}_2 &= -A_2 + w_2 \end{aligned} \tag{5.3}$$

with $\theta_1(t) = \theta + \frac{g}{\beta}(A_1(t) + I)$ and $\theta_2(t) = \theta + \frac{g}{\beta}(A_2(t) + I)$.

On the other hand, let us consider the system (2.1) with S as in (2.2). By a similar change of variables $w_1 = \beta u_1 - I$, $w_2 = \beta u_2 - I$, $A_1 = \beta a_1 - I$, $A_2 = \beta a_2 - I$ this system is diffeomorphic equivalent to

$$\begin{aligned} \dot{w}_1 &= -w_1 + \beta S(-w_2; \theta_1) - I, \\ \dot{w}_2 &= -w_2 + \beta S(-w_1; \theta_2) - I, \\ \tau \dot{A}_1 &= -A_1 + w_1, \\ \tau \dot{A}_2 &= -A_2 + w_2 \end{aligned} \tag{5.4}$$

with $\theta_1(t)$ and $\theta_2(t)$ as above. The threshold of S (rewritten as $S(x; \theta) = 1/(1 + e^{-r(x-\theta)})$) is θ .

As we can see, up to the specific expression of the gain function, Wilson's and the adaptation-LC models are equivalent. The reason Wilson's model shows preference to the escape mechanism instead of release (while for the adaptation-LC model the interval ranges for escape and release dynamics have equal length) resides in the asymmetric shape of \tilde{S} with respect to

its threshold. The threshold is Θ but the maximum gain is obtained at $\frac{\Theta}{\sqrt{3}} < \Theta$ ($\tilde{S}_{xx}(x; \Theta) = 0$ at $x = \frac{\Theta}{\sqrt{3}}$). The resulting behavior is similar to that of S as in (5.1) with $u_0 < 1/2$ ($S''(\theta) = 0$, $S(\theta) = u_0$, and $\theta < th$). The role of θ is played by $\frac{\Theta}{\sqrt{3}}$ and the corresponding value for u_0 is $\tilde{S}\left(\frac{\Theta}{\sqrt{3}}; \Theta\right) = 1/4$.

Remark 5.3. In fact, the difference between \tilde{S} and asymmetric S from (5.1) is more subtle. Take again $\gamma = 1$; the restriction of \tilde{S} on $(0, \infty)$ is invertible with inverse \tilde{F} defined on $(0, 1)$

by $\tilde{F}(u; \Theta) = \Theta \sqrt{\frac{u}{1-u}}$. In systems (5.3) and (5.4) the graph of \tilde{F}'_u

$\tilde{F}'_u(u; \theta_j) = \frac{\theta_j}{2(1-u)\sqrt{u(1-u)}}$ has a well-like shape similar to that of the graph of

$F'_u(u; \theta_j) = \frac{4u_0^2}{ru(2u_0-u)}$ if $u \in (0, u_0]$ and $\frac{4(1-u_0)^2}{r(1-u)(1-2u_0+u)}$ if $u \in (u_0, 1)$. However, \tilde{F}'_u

depends on θ_j (that implicitly means dependence on the slow variable) while F'_u does not. That explains why, for S as in (5.1), when they exist, the Hopf bifurcation points always come in pairs (and oscillations start at both points with the same frequency—see (3.5) and (3.6) in section 3); so release and escape oscillatory regimes (even if not equally balanced) always

coexist for (2.1). On the contrary, in Wilson’s model (5.2) the dependence of \tilde{F}'_u on the slow variable allows us to find a (reduced) parameter regime where only the escape mechanism is possible [31].

5.2. Competition models with nonlinear slow negative feedback

The local analysis pursued in section 3 shows that the uniform equilibrium point \mathbf{e}_I can lose its stability through either a Hopf bifurcation (at exactly two values I_{hb}^* and I_{hb}^{**}) or a pitchfork bifurcation (at exactly two values I_{pf}^* and I_{pf}^{**}). This result comes from the intersection of the

graph of F' (which has a well-like shape) with the straight horizontal lines $y = \frac{\beta}{1 + \frac{1}{\tau}}$ and $y = \beta - g$, respectively. This type of intersection restricts the possibilities to either $I_{hb}^* < I_{pf}^* < I_{pf}^{**} < I_{hb}^{**}$ or $I_{pf}^* < I_{hb}^* < I_{hb}^{**} < I_{pf}^{**}$. The first case corresponds to a feedback/adaptation-dominated neuronal competition model and ensures the existence of stable oscillations in (2.1). Moreover, these

appear with the same frequency $\omega = \frac{1}{\tau} \sqrt{\frac{g(\tau+1)}{\beta} - 1}$ at both values I_{hb}^* and I_{hb}^{**} , and they are due to two different mechanisms: escape (for larger values of I) and release (for lower values of I). Thus we conclude that in system (2.1) escape and release oscillatory regimes *always coexist*. The choice of asymmetric gain function with respect to its threshold helps to reduce one or another regime but cannot eliminate it completely.

Nevertheless there is a way to modify (2.1) such that the new obtained system shows preference to either the escape or release mechanism; moreover, as for Wilson’s model, in some parameter regime we can find only escape-based oscillations (or, vice versa, only release-based oscillations). In this sense we consider the neuronal competition model with nonlinear slow negative feedback

$$\begin{aligned} \dot{u}_1 &= -u_1 + S(I - \beta u_2 - g a_1), \\ \dot{u}_2 &= -u_2 + S(I - \beta u_1 - g a_2), \\ \tau \dot{a}_1 &= -a_1 + a_\infty(u_1), \\ \tau \dot{a}_2 &= -a_2 + a_\infty(u_2) \end{aligned} \tag{5.5}$$

with S as in (2.2) and

$$a_\infty(x; \theta_a) = 1 / (1 + e^{-r_a(x - \theta_a)}). \tag{5.6}$$

We obtain the following result, which is similar to Theorem 5.1.

Theorem 5.2. Consider the nonlinear term $a_\infty(x; \theta_a)$ defined by (5.6). If the gain function S satisfies $S(\theta + x) + S(\theta - x) = 1$, then system (5.5) with input I^* and slow equation nonlinearity $a_\infty(x; \theta_a)$ is diffeomorphic equivalent to system (5.5) with input $I = 2\theta + \beta + g - I^*$ and slow nonlinearity $a_\infty(x; 1 - \theta_a)$.

Proof. With the change of variables $u_1 = 1 - \tilde{u}_1, u_2 = 1 - \tilde{u}_2, a_1 = 1 - \tilde{a}_1, a_2 = 1 - \tilde{a}_2$, system (5.5) with input I^* and nonlinear term in the slow equation $a_\infty(x; \theta_a)$ takes the form (5.5) with input $(2\theta + \beta + g - I^*)$ and $a_\infty(x; 1 - \theta_a)$.

If $\theta_a = 1/2$, we have $a_\infty(x; \theta_a) = a_\infty(x; 1 - \theta_a)$, and thus the system (5.5) has the same type of solutions for any two values of input strength I_1 and I_1^* such that $\frac{1}{2}(I_1 + I_1^*) = \theta + \frac{\beta + g}{2}$. As for the case of linear adaptation (where the choice was $a_\infty(u) = u$), the intervals of I where the period of oscillations increases and decreases have the same length and are symmetric to the line

$$I = \theta + \frac{\beta + g}{2}.$$

The symmetry of the I - T bifurcation diagram can be destroyed by choosing $\theta_a \neq 1/2$. As numerical simulations of system (5.5) show, the choice of $\theta_a > 1/2$ leads to a preference of the system for the escape mechanism (decreasing T versus I). On the contrary, for $\theta_a < 1/2$ the system shows preference to the release mechanism (increasing T versus I).

For parameters $\beta = 1.1, g = 0.5, \tau = 100$, and $\theta = 0.2, r = 10$ for S and $r_a = 10$ and $\theta_a = 0.7$ for a_∞ , we plot in Figure 12 the bifurcation diagram of population activity u_1 versus the stimulus strength I and then the period T versus I . In Figure 12A we observe that the Hopf bifurcation point that existed for low value of I in case of linear adaptation disappears now. Instead we find a supercritical pitchfork bifurcation where stable nonuniform equilibrium points are born (they correspond to the winner-take-all case). The increasing branch of T versus I graph disappears while the decreasing branch is still present (Figure 12B). We find only four dynamical regimes (as opposed to the five described in Figure 3F and G): fusion (equal activity levels) for large and low input, winner-take-all, and oscillations with decreasing T as function of I for intermediate values of stimulus strength.

By choosing $\theta_a = 0.3$ the bifurcation diagrams in Figure 12 are virtually mirrored along the stimulus axis; in this case only the increasing I - T branch exists.

We explain these numerical results through an analytical approach. Similarly to the local analysis in section 3, we note that system (5.5) has a unique uniform equilibrium $\mathbf{e}_I = (u_I, u_I, a_\infty(u_I), a_\infty(u_I))$ for any real I . The value $u_I \in (0, 1)$ is defined by equation $I = F(u_I) + \beta u_I + g a_\infty(u_I)$ and decreases with a decrease in I ; moreover, $\lim_{I \rightarrow \infty} u_I = 1$ and $\lim_{I \rightarrow -\infty} u_I = 0$. The characteristic equation of the linearization matrix about \mathbf{e}_I is a product of two factors:

$$\lambda^2 + \lambda \left(1 + \frac{1}{\tau} + \frac{\beta}{F'(u_I)} \right) + \frac{1}{\tau} \left(1 + \frac{g a'_\infty(u_I) + \beta}{F'(u_I)} \right) = 0 \quad \text{and}$$

$$\lambda^2 + \lambda \left(1 + \frac{1}{\tau} - \frac{\beta}{F'(u_I)} \right) + \frac{1}{\tau} \left(1 + \frac{g a'_\infty(u_I) - \beta}{F'(u_I)} \right) = 0.$$

Thus two of the eigenvalues always have negative real part, while the other two show the type of stability for \mathbf{e}_I . Decreasing I , the stability

of \mathbf{e}_I is lost either through a pair of purely imaginary eigenvalues at $F'(u_I) = \beta / \left(1 + \frac{1}{\tau}\right)$, $F'(u_I) + ga'_{\infty}(u_I) > \beta$ or through a zero eigenvalue at $F'(u_I) + ga'_{\infty}(u_I) = \beta$ and $F'(u_I) > \beta / \left(1 + \frac{1}{\tau}\right)$.

Assume now that θ_a is greater than 1/2 and close to 1. For large I the corresponding fixed point \mathbf{e}_I has u_I close to 1 and in the vicinity of θ_a . Since this is the steeper (almost linear) part of

a_{∞} , we can approximate $a_{\infty}(u_I) \approx ku_I$. The condition $F'(u_I) = \beta / \left(1 + \frac{1}{\tau}\right)$,

$F'(u_I) > \beta - ga'_{\infty}(u_I) = \beta - gk$, can be attained (at least for adaptation-dominated systems) and stable oscillations occur. On the other hand, for small I , the fixed point \mathbf{e}_I has u_I close to 0 and further away from θ_a . The function a_{∞} is almost constant there, so $a'_{\infty}(u_I) \approx 0$. Then

$F'(u_I) + ga'_{\infty}(u_I) \approx \beta > \beta / \left(1 + \frac{1}{\tau}\right)$ and the stability of \mathbf{e}_I is lost through a zero eigenvalue (a pitchfork bifurcation).

Remark 5.4. We note that the choice of $\theta_a > 1/2$ sufficiently close to 1 helps the slow variable for the suppressed population, say, a_1 , to change faster than the slow variable for the dominant population, say, a_2 . Since $a_{\infty}(u_1)$ is approximately constant to zero and $a_{\infty}(u_2)$ falls onto the linear part of the sigmoid, a_1 decays almost exponentially according to $\tau \dot{a}_1 \approx -a_1$ while a_2 grows more slowly according to $\tau \dot{a}_2 \approx -a_2 + ku_2$. The input-output function of the suppressed population changes faster, favoring escape. An opposite effect is obtained for $\theta_a < 1/2$.

6. Discussion

We investigated a class of competition models that describe rhythmic (alternating) phenomena that arise in a range of neural contexts including perception of ambiguous sensory stimuli (such as binocular rivalry) and motor coordination (as in CPGs). These models rely on mutual inhibition between populations of neurons and a slow process in the form of spike frequency adaptation and/or synaptic depression, and they have the following commonalities [31].

A decrease in the strength of the input to the noise-free system leads to five possible types of dynamics: (i) at high values of input strength both competing populations are active at equal levels; (ii) by decreasing the input strength the system enters an oscillatory regime with the oscillation period increasing as input decreases; (iii) then for lower input the system is in a winner-take-all regime where only one population is dominant while the other is suppressed forever; (iv) continuing to decrease the input strength, the system oscillates again; in this region the oscillation period decreases as the input decreases; (v) at low values of input, oscillations disappear and both competing populations are inactive at an equal level. In addition, for weak inhibition the winner-take-all regime does not occur; however, the period of oscillations still depends on the input strength in a nonmonotonic fashion.

In a computational study of a model similar to (2.1), the authors of [23] also report transitions between simultaneous activity (single equilibrium), oscillations, and winner-take-all. The bifurcation diagram (Figure 4) in the parameter plane (I, β) resembles Figure 9 in [23]. However, Moldakarimov et al. were interested mostly in how the system's dynamics changes with inhibition strength (an internal parameter of the system) and not with stimulus strength. By analyzing the influence of stimulus on the oscillations' frequency/period, we provide a refined characterization of possible behaviors in this class of competition models.

The five dynamical regimes mentioned above were illustrated in Figure 3 for system (2.1), our choice as a particular example. Despite the fact that it has some limitations such as a lack of recurrent excitation, a symmetric gain function, and a nonsaturating $a_\infty(u)$, system (2.1) has the advantage of being simple enough to allow for a thorough analytical investigation while still displaying the dynamical characteristics found in a larger class of models. Thus, for (2.1) we proved the existence of oscillations and we showed that they are antiphase as expected for a network of two competing populations. Moreover, by considering the period of oscillations T as a function of input strength I , we proved that the I - T graph is nonmonotonic. We associated the increasing I - T branch with a release mechanism and the decreasing branch with an escape mechanism. Release occurs for lower values of I . It means that during oscillation the dominant population loses control due to accumulating slow negative feedback and it becomes unable to suppress its competitor; consequently the latter becomes active and thereby takes the role of suppressor. On the contrary, escape occurs for higher values of I and it means that the suppressed population regains control on its own, starts to inhibit its competitor, and forces it into the down state. Moreover, using singular perturbation techniques, we characterized in the limiting case the conditions for occurrence of winner-take-all dynamics at intermediate values of stimulus strength.

Our presumption is that the potential for alternation of percepts depends on neuronal competition. If competition were significantly reduced or eliminated (say, effectively making β very small in the model), alternations would not occur in the presence of a stimulus. That is, we suppose that an isolated population would not oscillate. To satisfy this constraint we have disallowed recurrent excitation in (2.1): this precludes oscillations in an isolated population for any input value I . Perhaps for this goal the complete elimination of recurrent excitation is an extreme way to satisfy the constraint. Alternatively, we could consider systems with fast equations of the form $\dot{u}_j = -u_j + S(I + \alpha u_j - \beta u_k - g a_j)$ and allow for some recurrent excitation

but not strong enough to let an isolated population oscillate (e.g., take $\alpha < \left(1 + \frac{1}{\tau}\right) / S'(\theta)$). This modification, however, does not affect our conclusion on the nonmonotonicity of the period of oscillations versus input strength curve (not shown): both “release” and “escape” branches still appear.

Other modifications of (2.1) that favor either release or escape as responsible for oscillations were discussed in section 5. One extension of (2.1) allows the gain function to be asymmetric with respect to the threshold. This maintains one of the two oscillatory regimes while reducing the other one. A different rendition of (2.1) invokes a nonlinear slow negative feedback (a sigmoidal-shaped $a_\infty(u)$) and completely eliminates one of the two regimes. The existence of the saturating branches for a sigmoidal $a_\infty(u)$ introduces an asymmetry in the system; thus under some specific conditions either the suppressed population recovers from slow negative feedback faster than the dominant population accumulates its own negative feedback (favoring escape, see Figure 12), or the reverse occurs. Interestingly, adding noise to these specially designed models, we automatically recover the nonmonotonicity of the period versus input curve [31].

Oscillations in mutually inhibitory neuronal networks based on fast-slow dynamics [27] as well as the terms “release” and “escape” [36,32] were previously discussed for neuronal networks in the presence of local autocatalysis. The autocatalysis was either an intrinsic process (like voltage-gated persistent inward currents) or a synaptic process (like intrapopulation recurrent excitation). Other models assumed networks of excitatory cells interacting through a global inhibitory feedback that typically produce the winner-take-all dynamics; the inhibition was dynamic with a slow time-scale and induced more complicated oscillatory patterns with one cell being active for a while and then spontaneously turning off and allowing another one

to take over [8]. Contrary to these examples, there is no autocatalysis in the neuronal competition models we investigate here. Instead the alternation is a combined result of two processes: mutual inhibition that acts effectively as a fast positive feedback (disinhibition) and a slow negative feedback (adaptation, but that could alternatively be synaptic depression).

Acknowledgments

We thank Sukbin Lim for helpful discussions.

The work of this author was supported by the Romanian grants CNCSIS AT55 and PNCDI-2 11-039/2007.

The work of the second author was supported by NIH grant EY07-158-03. The work of the third author was supported by the Swartz Foundation.

The work of this author was supported by the Swartz Foundation.

Appendix A. Normal form for Hopf bifurcation

To construct the normal form for the Hopf bifurcation, in section 3 we use the expansion of $S^{(k)}(F(u_I))$, $k = 1, 2, 3, \dots$, with respect to ε . That is obtained as follows: take, for example,

$$f_1(I) \stackrel{\text{def}}{=} S'(F(u_I)) = f_1(I^* + \varepsilon^2 \alpha) = f_1(I^*) + f_1'(I^*) \varepsilon^2 \alpha + \mathcal{O}(\varepsilon^4).$$

Here $f_1(I^*) = S'(F(u^*)) = 1/F'(u^*) = \left(1 + \frac{1}{\tau}\right) / \beta$ and $f_1'(I) = S''(F(u_I)) \cdot F'(u_I) \cdot du_I/dI$.

Based on (3.2), $f_1'(I) = S''(F(u_I)) \cdot F'(u_I) / (\beta + g + F'(u_I))$. On the other hand, since $u \equiv S(F(u))$, we have $1 \equiv S'(F(u)) \cdot F'(u)$, and further $0 \equiv S''(F(u)) \cdot F'(u)^2 + S'(F(u)) \cdot F''(u)$, i.e., $S''(F(u)) = -F''(u)/F'(u)^3$. Therefore,

$$f_1(I) = \frac{1 + 1/\tau}{\beta} - \frac{F''(u^*)}{F'(u^*)^2 (\beta + g + F'(u^*))} \varepsilon^2 \alpha + \mathcal{O}(\varepsilon^4).$$

Similarly, we compute

$$f_2(I) \stackrel{\text{def}}{=} S''(F(u_I)) = f_2(I^* + \varepsilon^2 \alpha) = f_2(I^*) + \mathcal{O}(\varepsilon^2) = -\frac{F''(u^*)}{F'(u^*)^3} + \mathcal{O}(\varepsilon^2)$$

and $f_3(I) \stackrel{\text{def}}{=} S'''(F(u_I)) = f_3(I^* + \varepsilon^2 \alpha) = f_3(I^*) + \mathcal{O}(\varepsilon^2) = S'''(F(u^*)) + \mathcal{O}(\varepsilon^2)$. From $S''(F(u)) = -F''(u)/F'(u)^3$ we obtain $S'''(F(u)) = [3F''(u)^2 - F''(u) \cdot F'''(u)]/F'(u)^5$, so

$$f_3(I) = \frac{3F''(u^*)^2 - F''(u^*) \cdot F'''(u^*)}{F'(u^*)^5} + \mathcal{O}(\varepsilon^2).$$

Normal form

Let us now present the main steps in the algorithm for the construction of the normal form starting with

$$L_0 V_0 = \varepsilon [\mathcal{B}(V_0, V_0) - L_0 V_1] + \varepsilon^2 [C(V_0, V_0, V_0) + 2\mathcal{B}(V_0, V_1) + \Lambda V_0 - L_0 V_2] + \mathcal{O}(\varepsilon^3). \tag{A.1}$$

In the limit $\varepsilon \rightarrow 0$, the vector V_0 is a solution of the linear system $L_0 V_0 = 0$ with two eigenvalues $\lambda_{1,2}$ of negative real part and two purely imaginary eigenvalues $\lambda_{3,4} = \pm i\omega$. Thus V_0 belongs to the center manifold; i.e., for an eigenvector $\xi \in \mathbb{C}^4$ of \mathcal{A}_0 that satisfies $\mathcal{A}_0 \xi = i\omega \xi$ say,

$$\xi = (-\tau\omega + i, \tau\omega - i, i, -i)^T, \tag{A.2}$$

the solution V_0 takes the form

$$V_0(t) = w(t) \xi e^{i\omega t} + \bar{w}(t) \bar{\xi} e^{-i\omega t}.$$

However, since $L_0 V_0 = \mathcal{O}(\varepsilon)$, $w(t)$ is ε -dependent, and it can be written in slow time $s = \varepsilon^2 t$ as

$w = w(s)$. In the singular perturbation expansion, $w(s) = w(s)|_{\varepsilon=0} + \frac{dw}{ds}|_{\varepsilon=0} \varepsilon^2 t + \mathcal{O}(\varepsilon^4)$. With

notation $Z = w(s)|_{\varepsilon=0}$, $Z' = \frac{dw}{ds}|_{\varepsilon=0}$, and so on (here ' stands for the derivative with respect to the slow time), we have $w = Z + \varepsilon^2 t Z' + \mathcal{O}(\varepsilon^4)$ and

$$V_0 = \left(Z \xi e^{i\omega t} + \bar{Z} \bar{\xi} e^{-i\omega t} \right) + \varepsilon^2 t \left(Z' \xi e^{i\omega t} + \bar{Z}' \bar{\xi} e^{-i\omega t} \right) + \mathcal{O}(\varepsilon^4).$$

Then we compute $L_0 (te^{i\omega t} \xi) = e^{i\omega t} \xi$, $L_0 (te^{-i\omega t} \bar{\xi}) = e^{-i\omega t} \bar{\xi}$ and $\mathcal{B}(\xi e^{i\omega t}, \xi e^{i\omega t}) = \frac{1}{2} B b^2 p e^{2i\omega t}$,

$\mathcal{B}(\bar{\xi} e^{-i\omega t}, \bar{\xi} e^{-i\omega t}) = \frac{1}{2} B \bar{b}^2 \bar{p} e^{-2i\omega t}$, $\mathcal{B}(\xi e^{i\omega t}, \bar{\xi} e^{-i\omega t}) = \frac{1}{2} B |b|^2 p$, where $b = \beta\tau\omega + i(g - \beta)$ and $p = (1, 1, 0, 0)^T$. Equation (A.1) becomes

$$\begin{aligned} L_0 V_1 = & \frac{1}{2} Z^2 B b^2 p e^{2i\omega t} \\ & + \frac{1}{2} \bar{Z}^2 B \bar{b}^2 \bar{p} e^{-2i\omega t} \\ & + Z \bar{Z} B |b|^2 p \\ & + \varepsilon \left[-Z' \xi e^{i\omega t} - \bar{Z}' \bar{\xi} e^{-i\omega t} + C(V_0, V_0, V_0) + 2\mathcal{B}(V_0, V_1) + \Lambda V_0 - L_0 V_2 \right] + \mathcal{O}(\varepsilon^2), \end{aligned}$$

so we look for solutions V_1 of the form

$$V_1 = w^2 \xi_1 e^{2i\omega t} + 2w \bar{w} \xi_2 + \bar{w}^2 \bar{\xi}_3 e^{-2i\omega t} = Z^2 \xi_1 e^{2i\omega t} + 2Z \bar{Z} \xi_2 + \bar{Z}^2 \bar{\xi}_3 e^{-2i\omega t} + \mathcal{O}(\varepsilon^2).$$

From the singular perturbation expression we determine $\xi_1 = \frac{1}{2} B b^2 (2i\omega I - \mathcal{A}_0)^{-1} p$, $\xi_2 = -\frac{1}{2} B |b|^2 \mathcal{A}_0^{-1} p$ and $\xi_3 = \zeta_1^-$, that is,

$$\xi_1 = \frac{B b^2 \psi}{2 |\psi|^2} (1 + 2i\tau\omega, 1 + 2i\tau\omega, 1, 1)^T, \quad \xi_2 = \frac{B |b|^2}{2 \left[1 + \left(\frac{g}{\beta} + 1\right) \left(1 + \frac{1}{\tau}\right) \right]} (1, 1, 1, 1)^T,$$

where $\psi = 1 - 4\omega^2\tau + \left(\frac{g}{\beta} + 1\right) \left(1 + \frac{1}{\tau}\right) - 4i\omega(\tau + 1)$.

Then we compute $C(V_0, V_0, V_0)$, $\mathcal{B}(V_0, V_1)$ and $\Lambda V_0 = -\alpha A \left(Z b e^{i\omega t} + \bar{Z} \bar{b} e^{-i\omega t} \right) q + \mathcal{O}(\varepsilon^2)$ with $q = (1, -1, 0, 0)^T$ and obtain

$$L_0 V_2 = - \left(Z' \xi + \alpha A Z b q \right) e^{i\omega t} + Z^2 \bar{Z} b^2 \bar{b} q e^{i\omega t} \left(-\frac{D}{2} + \frac{(\beta + g) B^2}{1 + \left(\frac{g}{\beta} + 1\right) \left(1 + \frac{1}{\tau}\right)} + \frac{B^2 (\beta + g + 2i\beta\omega\tau) \psi}{2 |\psi|^2} \right) + e^{3i\omega t} (\dots) + cc + \mathcal{O}(\varepsilon).$$

In order for the solution V_2 to exist, the right-hand side of the above equation should be orthogonal on the eigenvectors of the adjoint operator $L_0^* = -\frac{d}{dt} - \mathcal{A}_0^T$ on the space of periodic solutions $V(t) = V \left(t + \frac{2\pi}{\omega} \right)$ with inner product

$$\langle V, W \rangle = \frac{\omega}{2\pi} \int_0^{\frac{2\pi}{\omega}} \sum_{i=1}^4 v_i(t) \bar{w}_i(t) dt, \quad V = (v_i)_{i=1,4}^T, \quad W = (w_i)_{i=1,4}^T.$$

That means the right-hand side should be orthogonal on $\{\eta e^{i\omega t}, \eta^- e^{-i\omega t}\}$ with η solution of $\mathcal{A}_0^T \eta = -i\omega \eta$ and $\zeta \cdot \eta^- = 1$; that is,

$$\eta = -\frac{1}{4\omega\tau} (1, -1, -1 - i\omega\tau, 1 + i\omega\tau)^T.$$

We obtain the normal form $Z' = \alpha A \varphi Z - \mathcal{L} Z^2 \bar{Z}$ with \mathcal{L} as in Theorem 3.2.

By rescaling $I - I^* = \varepsilon^2 \alpha$ and $z(t) = \varepsilon Z(\varepsilon^2 t) = \varepsilon Z(s)$, we have $\dot{z} = dz/dt = \varepsilon \frac{dZ}{ds} \frac{ds}{dt} = \varepsilon^3 Z'$; the above differential equation becomes exactly (3.11).

First Lyapunov coefficient

We would like to determine sufficient conditions for the Hopf bifurcation to be supercritical, i.e., for $\text{Re}(\mathcal{L}) > 0$.

We now use inequality (3.3) to show that the first term in the sum that defines \mathcal{L} has positive real part:

$$\begin{aligned}
 & \operatorname{Re}\left(\varphi\psi\left(\frac{\beta+g}{2}+i\beta\omega\tau\right)\right) \\
 &= (2\beta g)\tau \\
 &+ \frac{1}{4}\left(7g^2+5\beta g-6\beta^2\right) \\
 &+ \frac{1}{4\tau}\left(7g^2-6\beta g+3\beta^2\right) > 2\beta^2 \\
 &- 2\beta g \\
 &+ \frac{1}{4}\left(7g^2+5\beta g-6\beta^2\right) \\
 &+ \frac{1}{4\tau}\left(7g^2-6\beta g+3\beta^2\right) \\
 &= \frac{1}{4}\left(7g^2-3\beta g+2\beta^2\right) \\
 &+ \frac{1}{4\tau}\left(7g^2-6\beta g+3\beta^2\right) > 0.
 \end{aligned}
 \tag{A.3}$$

For the second term, (3.3) implies

$$l_1 = \frac{2(\beta+g)}{1+\left(\frac{g}{\beta}+1\right)\left(1+\frac{1}{\tau}\right)} = \frac{2}{\frac{1}{\beta+g} + \frac{1}{F'(u^*)}} > \left(1 + \frac{1}{\tau+1}\right) F'(u^*) > F'(u^*).$$

Therefore, the real part of the second term satisfies

$$\beta\tau^2\omega^2|\varphi|^2B^2\left(l_1 - \frac{D}{B^2}\right) > \beta\tau^2\omega^2|\varphi|^2B^2F'(u^*)\left(\frac{F'(u^*)F''(u^*)}{F''(u^*)^2} - 2\right).
 \tag{A.4}$$

Appendix B. Normal form for pitchfork bifurcation

The construction of this normal form follows similar steps to those in section 3.1 and Appendix

A. Here $F'(u^0) = \beta - g$ with $u^0 \in \{u_{pf}^*, u_{pf}^{**}\}$ and $I^0 \in \{I_{pf}^*, I_{pf}^{**}\}$.

The operators $\mathcal{B}, \mathcal{C}, \Lambda$, and L_0 are defined in the same way as in section 3.1 with coefficients A, B, D as in (3.10). However, the derivatives of F at the bifurcation point u^0 take different

values, so $S'(F(u_t)) = 1/(\beta - g) + \alpha A \varepsilon^2 + \mathcal{O}(\varepsilon^4)$, $S''(F(u_t)) = B + \mathcal{O}(\varepsilon^2)$, and

$S'''(F(u_t)) = D + \mathcal{O}(\varepsilon^2)$ with A, B , and D evaluated at either u_{pf}^* or u_{pf}^{**} . The matrix of the linearized system is now

$$\mathcal{A}_0 = \begin{pmatrix} -1 & -\frac{\beta}{\beta-g} & -\frac{g}{\beta-g} & 0 \\ -\frac{\beta}{\beta-g} & -1 & 0 & -\frac{g}{\beta-g} \\ \frac{1}{\tau} & 0 & -\frac{1}{\tau} & 0 \\ 0 & \frac{1}{\tau} & 0 & -\frac{1}{\tau} \end{pmatrix}$$

and has a zero eigenvalue. Therefore, we find an eigenvector ζ ($\mathcal{A}_0 \zeta = 0$) and an eigenvector η of the adjoint matrix ($\mathcal{A}_0^T \eta = 0$) such that $\zeta \cdot \eta = 1$. They are

$$\xi = (1, -1, 1, -1)^T, \quad \eta = \frac{1}{2(\beta - g(\tau + 1))} (\beta - g, -\beta + g, -\tau g, \tau g)^T.$$

With the perturbation $I - I^o = \varepsilon^2 \alpha$, $V(t) = \varepsilon V_0(t) + \varepsilon^2 V_1(t) + \varepsilon^3 V_2(t) + \dots$, we obtain that V_0 belongs to the eigenspace, that is, $V_0 = w(t)\zeta$. The expansion with respect to the slow time ($s = \varepsilon^2 t$, $w = w(s)$, $Z = w(s)|_{\varepsilon=0}$, etc.) implies $V_0 = \left(Z + \varepsilon^2 t Z' + \mathcal{O}(\varepsilon^4) \right) \xi$ and

$$L_0 V_1 = Z^2 \mathcal{B}(\xi, \xi) + \varepsilon \left[-Z' \xi + Z^3 C(\xi, \xi, \xi) + 2\mathcal{B}(V_0, V_1) + Z \Lambda \xi - L_0 V_2 \right] + \mathcal{O}(\varepsilon^2).$$

The vector V_1 is chosen to be of the form $V_1 = w^2 \xi_1 = Z^2 \xi_1 + \mathcal{O}(\varepsilon^2)$ with ξ_1 orthogonal on η . It results in $\xi_1 = -\mathcal{A}_0^{-1} \mathcal{B}(\xi, \xi)$, i.e., $\xi_1 = \frac{B^2(\beta - g)^3}{4\beta} (1, 1, 1, 1)^T$. The normal form is

$$Z' = (\Lambda \xi \cdot \eta) Z + [C(\xi, \xi, \xi) \cdot \eta + 2\mathcal{B}(\xi, \xi_1) \cdot \eta] Z^3.$$

From $\Lambda \xi = \alpha A(\beta - g)\mathbf{q}$, $C(\xi, \xi, \xi) = \frac{D}{6}(\beta - g)^3 \mathbf{q}$, $\mathcal{B}(\xi, \xi_1) = -\frac{B^2}{8\beta}(\beta - g)^4(\beta + g)\mathbf{q}$ (where $\mathbf{q} = (1, -1, 0, 0)^T$), and by rescaling $I - I^o = \varepsilon^2 \alpha$ and $z(t) = \varepsilon Z(\varepsilon^2 t) = \varepsilon Z(s)$, we obtain exactly (3.15).

Appendix C. Additional material

To illustrate system (2.1)'s dynamics under the *escape* and *release* mechanisms we run numerical simulations in XPPAUT [7,9] with S as in (2.2), $r = 10$, $\theta = 0.2$, and parameters $\beta = 1.1$, $g = 0.5$, $\tau = 100$ as in Figure 3F. Then in the fast plane (u_1, u_2) we obtain the trajectory of the point on the rivalry limit cycle: the point is drawn as a black thick dot; the u_1 -nullcline is colored in red, and the u_2 -nullcline is colored in blue.

70584_01.gif [3.7MB] illustrates the escape mechanism for $I = 1.5$.

70584_02.gif [3.8MB] illustrates the release mechanism for $I = 0.5$.

The small black square corresponds to the slow plane (a_1, a_2) , where we included in green the projection of the limit cycle trajectory. This picture shows how the slow negative feedback accumulates for the dominant population and then how it recovers for the suppressed population (e.g., if u_1 is ON and u_2 is OFF, then a_1 increases and a_2 decreases). Then the cycle repeats.

REFERENCES

- [1]. Andrews TJ, Purves D. Similarities in normal and binocular rivalrous viewing. Proc. Natl. Acad. Sci. USA 1997;94:9905–9908. [PubMed: 9275224]
- [2]. Blake R. A neural theory of binocular rivalry. Psychol. Rev 1989;96:145–167. [PubMed: 2648445]
- [3]. Brascamp JW, van Ee R, Noest AJ, Jacobs RH, van den Berg AV. The time course of binocular rivalry reveals a fundamental role of noise. J. Vis 2006;6:1244–1256. [PubMed: 17209732]
- [4]. Curtu R, Ermentrout B. Oscillations in a refractory neural net. J. Math. Biol 2001;43:81–100. [PubMed: 12120869]

- [5]. Curtu R, Ermentrout B. Pattern formation in a network of excitatory and inhibitory cells with adaptation. *SIAM J. Appl. Dyn. Syst* 2004;3:191–231.
- [6]. Calabrese, RL. Half-center oscillators underlying rhythmic movements. In: Arbib, MA., editor. *The Handbook of Brain Theory and Neural Networks*. MIT Press; Cambridge, MA: 1995. p. 444-447.
- [7]. Ermentrout, B. 2006. <http://www.math.pitt.edu/~bard/xpp/xpp.html>
- [8]. Ermentrout B. Complex dynamics in winner-take-all neural nets with slow inhibition. *Neural Networks* 1992;5:415–431.
- [9]. Ermentrout, B. *Software Environ. Tools*. Vol. 14. SIAM; Philadelphia: 2002. *Simulating, Analyzing, and Animating Dynamical Systems: A Guide to XPPAUT for Researchers and Students*.
- [10]. Freeman AW. Multistage model for binocular rivalry. *J. Neurophysiol* 2005;94:4412–4420. [PubMed: 16148271]
- [11]. Getting, PA. Comparative analysis of invertebrate central pattern generators. In: Cohen, AH.; Rossignol, S.; Grillner, S., editors. *Neural Control of Rhythmic Movements in Vertebrates*. Wiley; New York: 1988. p. 101-127.
- [12]. Golubitsky, M.; Stewart, I. *The Symmetry Perspective: From Equilibrium to Chaos in Phase Space and Physical Space*. Birkhäuser; Basel: 2004.
- [13]. Grossberg S. Pattern formation by the global limits of a nonlinear competitive interaction in n dimensions. *J. Math. Biol* 1977;4:237–256. [PubMed: 894150]
- [14]. Guckenheimer, J.; Holmes, P. *Nonlinear Oscillations, Dynamical Systems, and Bifurcations of Vector Field*. Springer-Verlag; New York: 1983.
- [15]. Gurney K, Prescott TJ, Redgrave P. A computational model action selection in the basal ganglia (I): *A new functional anatomy*. *Biol. Cybernet* 2001;84:401–410.
- [16]. Kuznetsov, YA. *Elements of Applied Bifurcation Theory*. 2nd ed.. Springer-Verlag; New York: 1998.
- [17]. Laing CR, Chow CC. A spiking neuron model for binocular rivalry. *J. Comput. Neurosci* 2002;12:39–53. [PubMed: 11932559]
- [18]. Lee SH, Blake R, Heeger DJ. Traveling waves of activity in primary visual cortex during binocular rivalry. *Nat. Neurosci* 2005;8:22–23. [PubMed: 15580269]
- [19]. Levelt, WJM. *Psychological Studies, Minor Series*. Vol. 2. Mouton, The Hague, The Netherlands: 1968. *On Binocular Rivalry*.
- [20]. Logothetis NK, Leopold DA, Sheinberg DL. What is rivaling during binocular rivalry? *Nature* 1996;380:621–624. [PubMed: 8602261]
- [21]. Mao ZH, Massaquoi SG. Dynamics of winner-take-all competition in recurrent neural networks with lateral inhibition. *IEEE Trans. Neural Networks* 2007;18:55–69.
- [22]. Maynard Smith, J. *Models in Ecology*. Cambridge University Press; Cambridge, UK: 1974. p. 59-68.
- [23]. Moldakarimov S, Rollenhagen JE, Olson CR, Chow CC. Competitive dynamics in cortical responses to visual stimuli. *J. Neurophysiol* 2005;94:3388–3396. [PubMed: 15944239]
- [24]. Moreno-Bote R, Rinzel J, Rubin N. Noise-induced alternations in an attractor network model of perceptual bi-stability. *J. Neurophysiol* 2007;98:1125–1139. [PubMed: 17615138]
- [25]. Mueller TJ, Blake R. A fresh look at the temporal dynamics of binocular rivalry. *Biol. Cybernet* 1989;61:223–232.
- [26]. Polonsky A, Blake R, Braun J, Heeger DJ. Neuronal activity in human primary visual cortex correlates with perception during binocular rivalry. *Nat. Neurosci* 2000;3:1153–1159. [PubMed: 11036274]
- [27]. Rubin, J.; Terman, D. Geometric singular perturbation analysis of neuronal dynamics. In: Fiedler, B., editor. *Handbook of Dynamical Systems*. Vol. 2. Elsevier; Amsterdam: 2002. p. 93-146.
- [28]. Rubin N. Binocular rivalry and perceptual multi-stability. *Trends in Neurosci* 2003;26:289–291.
- [29]. Rubin, N.; Hupe, JM. Dynamics of perceptual bi-stability: Plaids and binocular rivalry compared. In: Alais, D.; Blake, R., editors. *Binocular Rivalry and Bistable Perception*. MIT Press; Cambridge, MA: 2004.
- [30]. Salinas E. Background synaptic activity as a switch between dynamical states in a network. *Neural Comput* 2003;15:1439–1475. [PubMed: 12816561]

- [31]. Shpiro A, Curtu R, Rinzel J, Rubin N. Dynamical characteristics common to neuronal competition models. *J. Neurophysiol* 2007;97:462–473. [PubMed: 17065254]
- [32]. Skinner FK, Kopell N, Marder E. Mechanisms for oscillation and frequency control in reciprocally inhibitory model neural networks. *J. Comput. Neurosci* 1994;1:69–87. [PubMed: 8792226]
- [33]. Taylor AL, Cottrell GW, Kristan WB Jr. Analysis of oscillations in a reciprocally inhibitory network with synaptic depression. *Neural Comput* 2002;14:561–581. [PubMed: 11860683]
- [34]. Tong F, Nakayama K, Vaughan JT, Kanwisher N. Binocular rivalry and visual awareness in human extrastriate cortex. *Neuron* 1998;21:753–759. [PubMed: 9808462]
- [35]. van Ooyen A. Competition in the development of nerve connections: A review of models. *Network: Comput. in Neural Syst* 2001;12:1–47.
- [36]. Wang X-J, Rinzel J. Alternating and synchronous rhythms in reciprocally inhibitory model neurons. *Neural Comput* 1992;4:84–97.
- [37]. Wilson HR. Computational evidence for a rivalry hierarchy in vision. *Proc. Natl. Acad. Sci. USA* 2003;100:14499–14503. [PubMed: 14612564]
- [38]. Wilson HR, Blake R, Lee SH. Dynamics of travelling waves in visual perception. *Nature* 2001;412:907–910. [PubMed: 11528478]

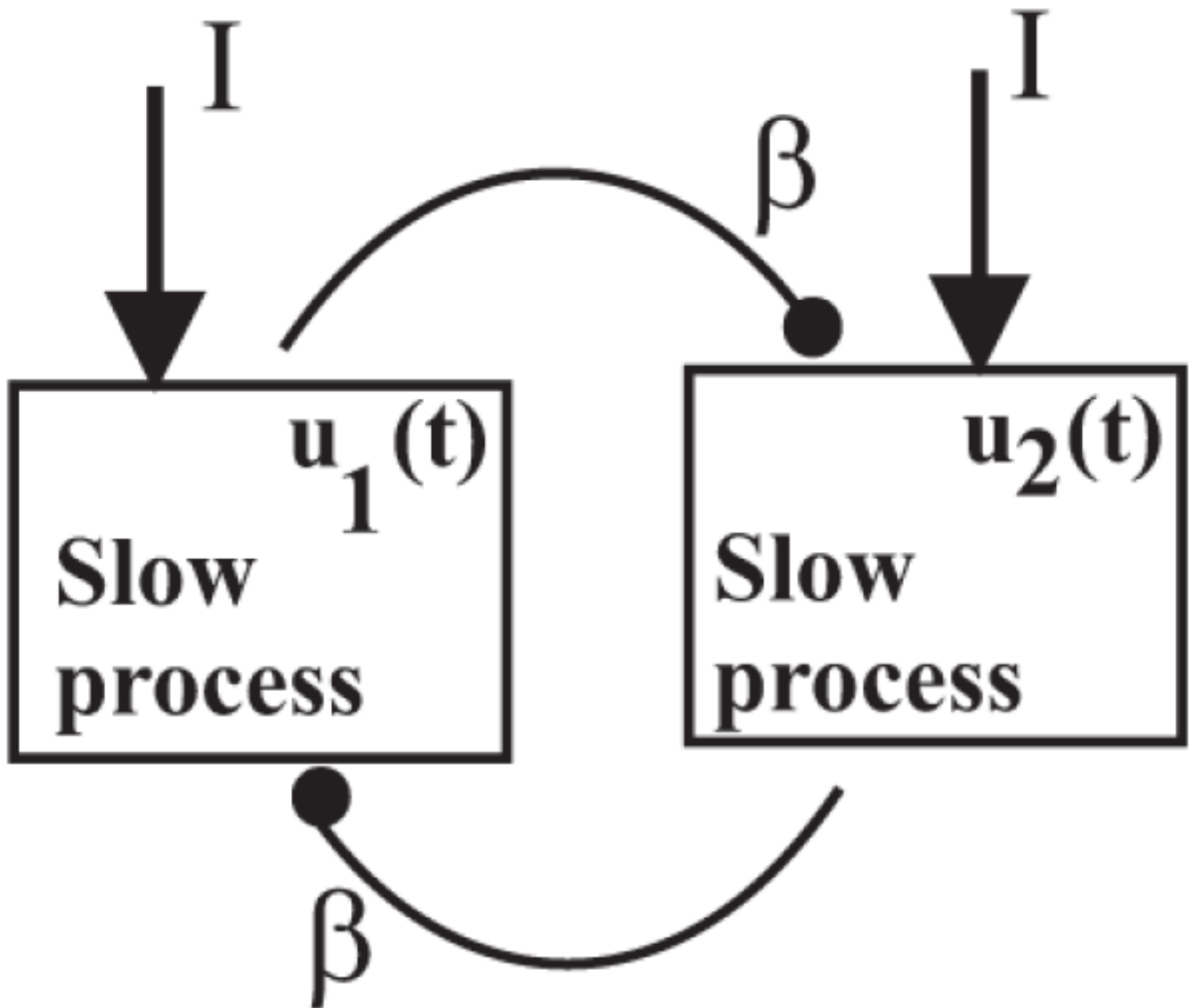


Figure 1.
Network architecture of neuronal competition model.

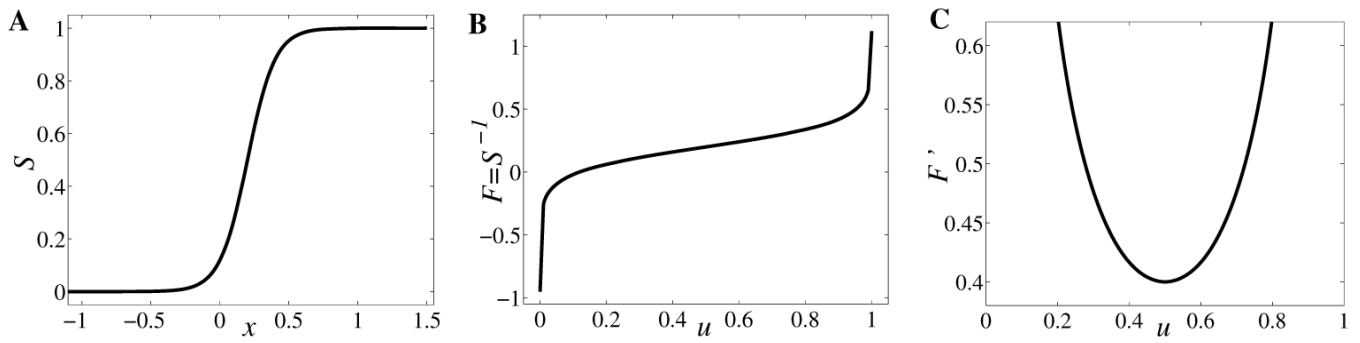


Figure 2.
Graphical representations of generic (A) gain function S ; (B) its inverse F ; and (C) first derivative F' .

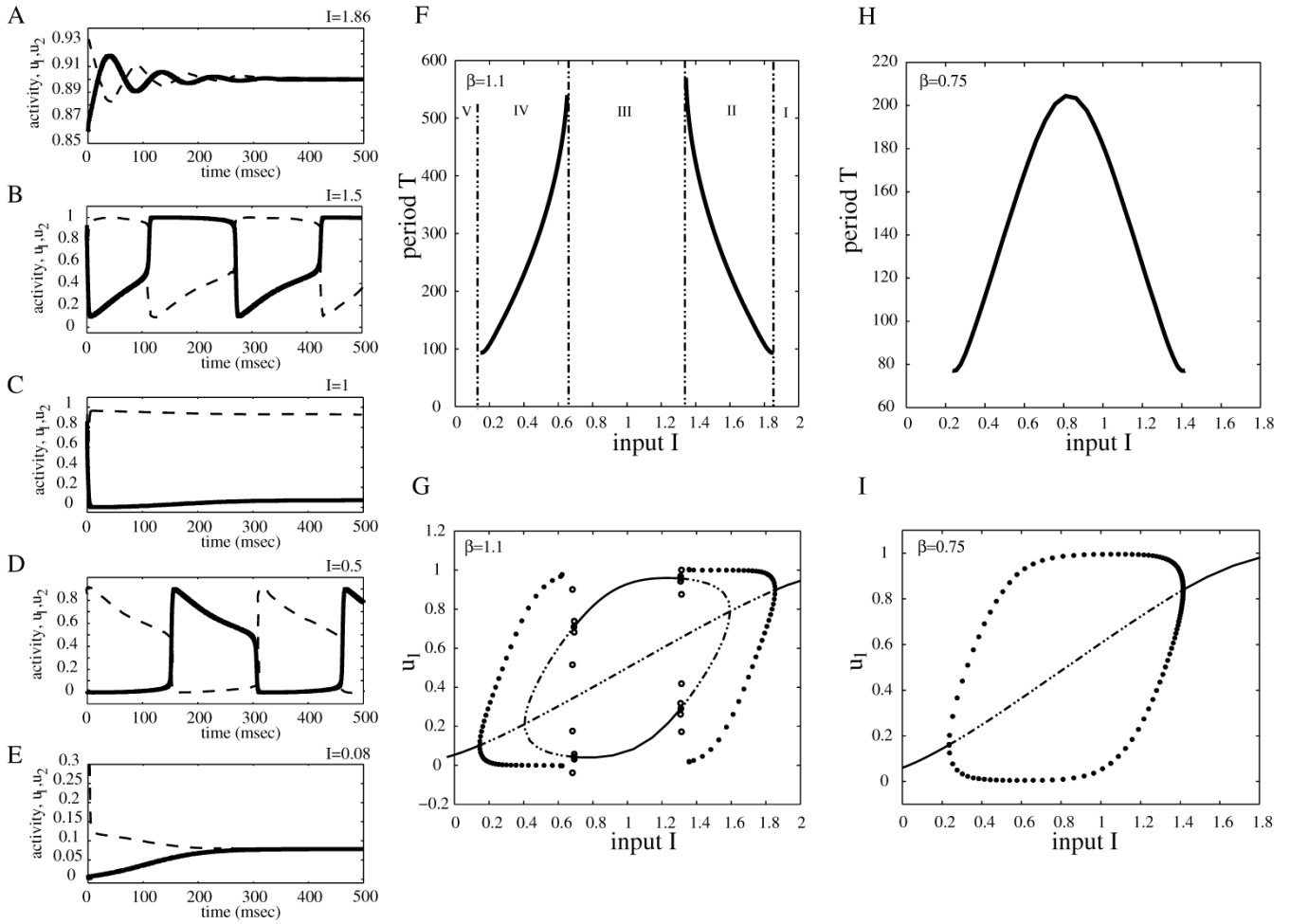


Figure 3. Bifurcation diagrams and examples of activity timecourses for neuronal competition model (2.1) with parameter values $g = 0.5$, $\tau = 100$, $r = 10$, $\theta = 0.2$, and $\beta = 1.1$ (A–G), respectively, $\beta = 0.75$ (H–I). Timecourses of u_1, u_2 corresponding to panel F for different values of I : (A) $I = 1.86$, (B) $I = 1.5$, (C) $I = 1$, (D) $I = 0.5$, and (E) $I = 0.08$. Bifurcation diagrams of period T of the network oscillation versus input strength I (F and H). Bifurcation diagram of population activity u_1 versus I (G and I).

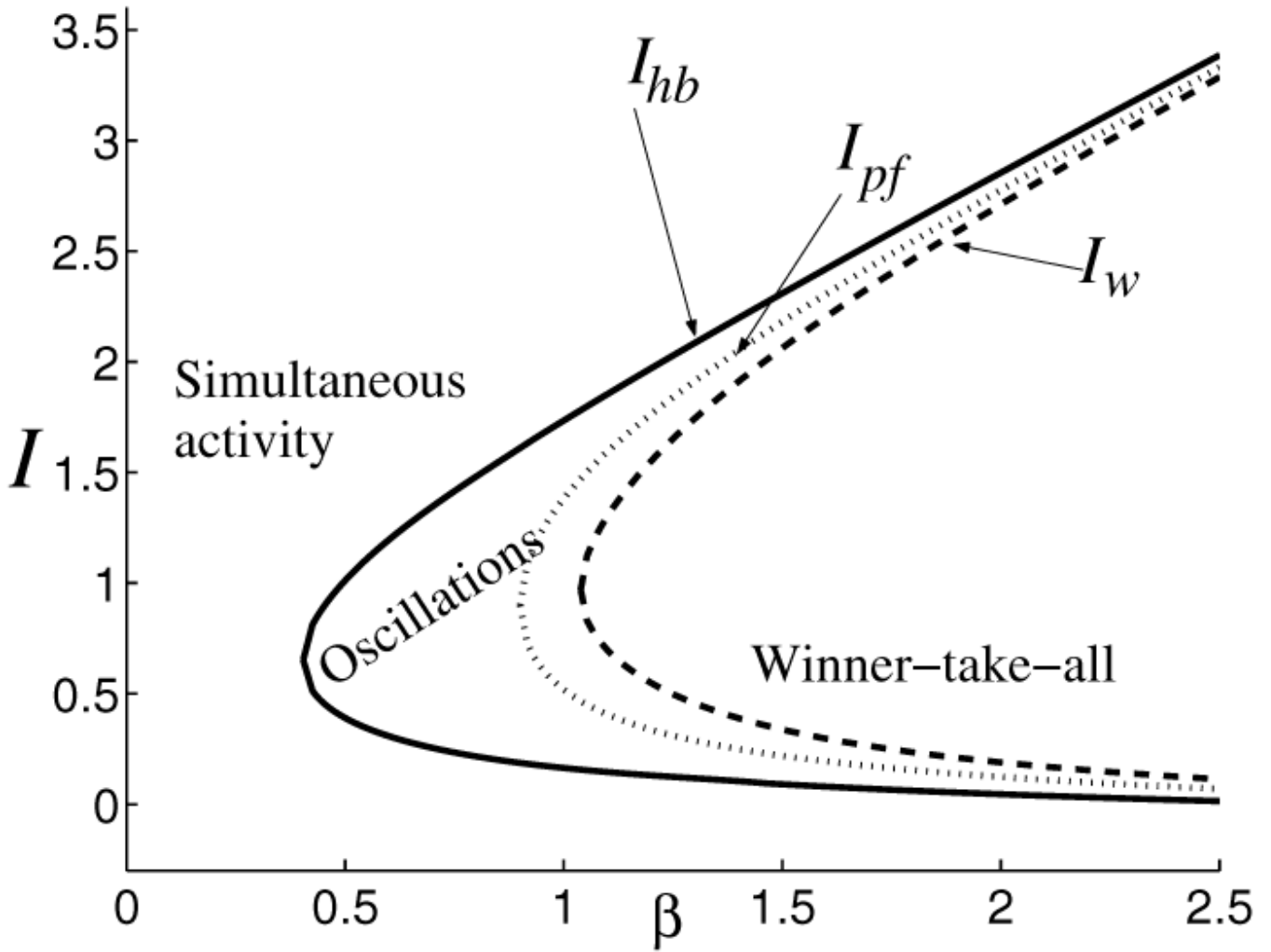


Figure 4. *Dynamical regimes in system (2.1) as inhibition strength β and stimulus strength I vary (other parameters are fixed: $g = 0.5$, $\tau = 100$, $r = 10$, $\theta = 0.2$). To the left of curve I_{hb} (solid line) the system has a unique stable equilibrium, and this satisfies $u_1 = u_2$ (simultaneous activity); in the region between curves I_{hb} and I_w (dashed line) the system oscillates; then to the right of I_w the system has a winner-take-all behavior (two stable and one unstable equilibria). The curve I_{pf} (dotted line) indicates a transition from one equilibrium to multiple equilibria in (2.1). While the attractor's type (limit cycle) does not change between I_{hb} and I_w , the number of equilibria does: we find one unstable equilibrium between I_{hb} , I_{pf} and three unstable equilibria between*

I_{pf} , I_w . The turning points of curves I_{hb} , I_{pf} , and I_w are obtained at $\beta = \frac{1+1/\tau}{S'(\theta)} = 0.404$, $\beta = g+1/S'(\theta) = 0.9$, and $\beta_{wta} = 1.0387$, respectively.

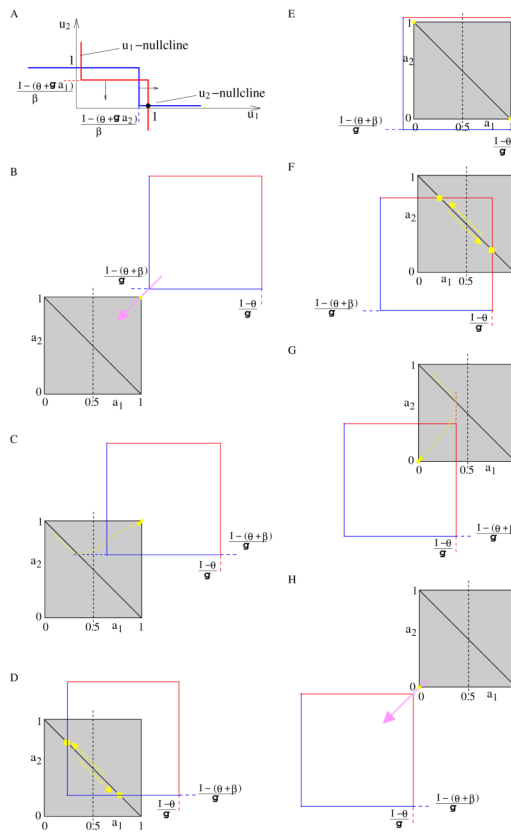


Figure 5. System (2.1)'s dynamics for large inhibition strength ($\beta/g > 1$) and Heaviside step function. (A) Nullclines in the plane of fast variables (u_1, u_2); (B–H) System's dynamics in the slow variables plane (a_1, a_2) for: (B) $I \geq \theta + \beta + g$; (C) $\theta + \beta + g/2 \leq I < \theta + \beta + g$; (D) $\theta + \beta < I < \theta + \beta + g/2$; (E) $\theta + g \leq I \leq \theta + \beta$; (F) $\theta + g/2 < I < \theta + g$; (G) $\theta \leq I \leq \theta + g/2$; (H) $I < \theta$.

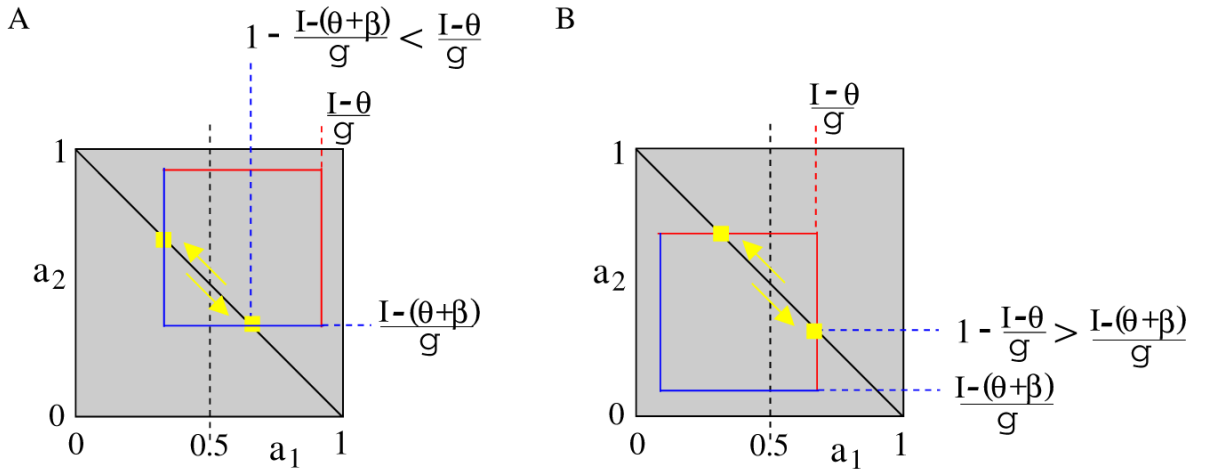


Figure 6. (A) *Escape* and (B) *release* mechanisms for low inhibition strength ($\beta/g < 1$) in system (2.1) with Heaviside step function.

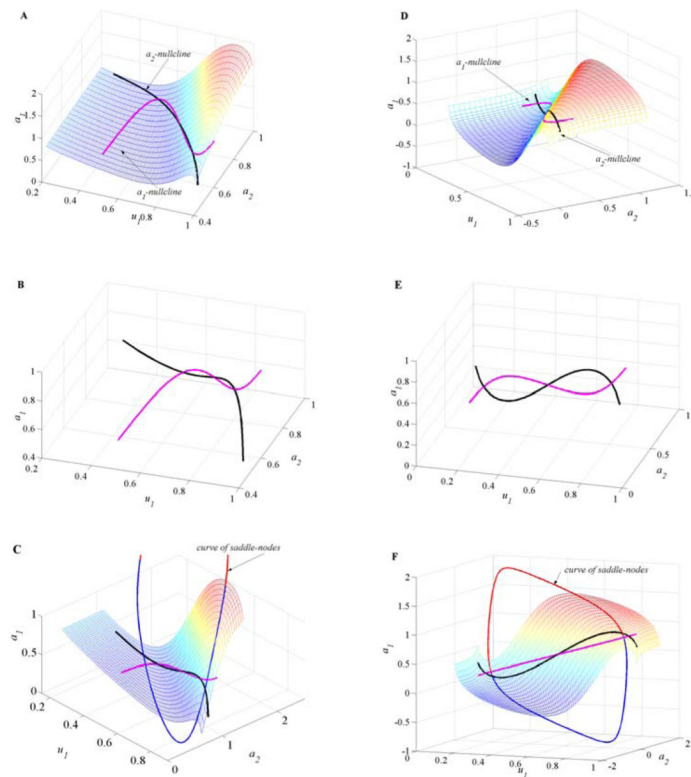


Figure 7. Projection of the slow manifold Σ on the space (u_1, a_1, a_2) . System (2.1)'s parameters are $\beta = 1.1$, $g = 0.5$, $\theta = 0.2$, $r = 10$, and $I = 1.5$ (A–C), respectively, $I = 1$ (D–F). The curve SN of saddle-nodes (jumping points) is represented in blue-red (C, F). Nullclines N_1 (magenta) and N_2 (black curve) intersect in three points for (B) $I = 1.5$ and (E) $I = 1$. However, either the equilibrium points can all lie on the middle branch of Σ (A), that is, inside the curve of saddle-nodes (C), or two equilibrium points can move to the lateral branches, outside of SN (D, F).

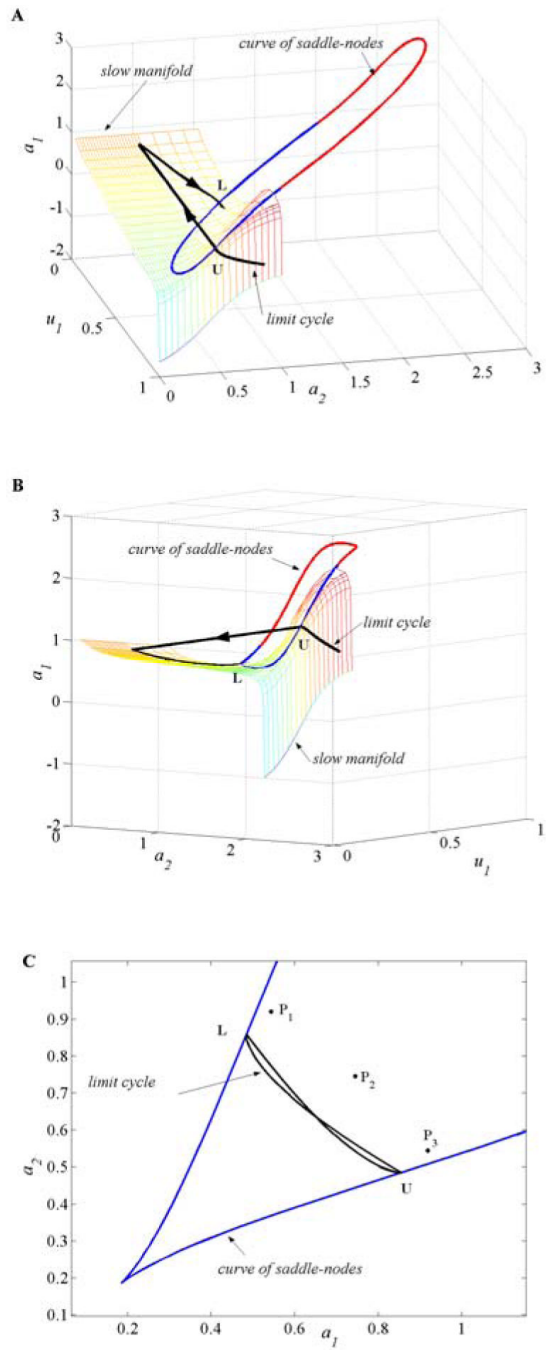


Figure 8. (A–B) Limit cycle solution and the slow manifold Σ for system (2.1) with parameters $I = 1.5$, $\beta = 1.1$, $g = 0.5$, $r = 10$, $\theta = 0.2$, and $\tau = 5000$. (C) The projection of the limit cycle on the slow plane (a_1, a_2) ; P_1 , P_2 , and P_3 are the projections of the equilibrium points.

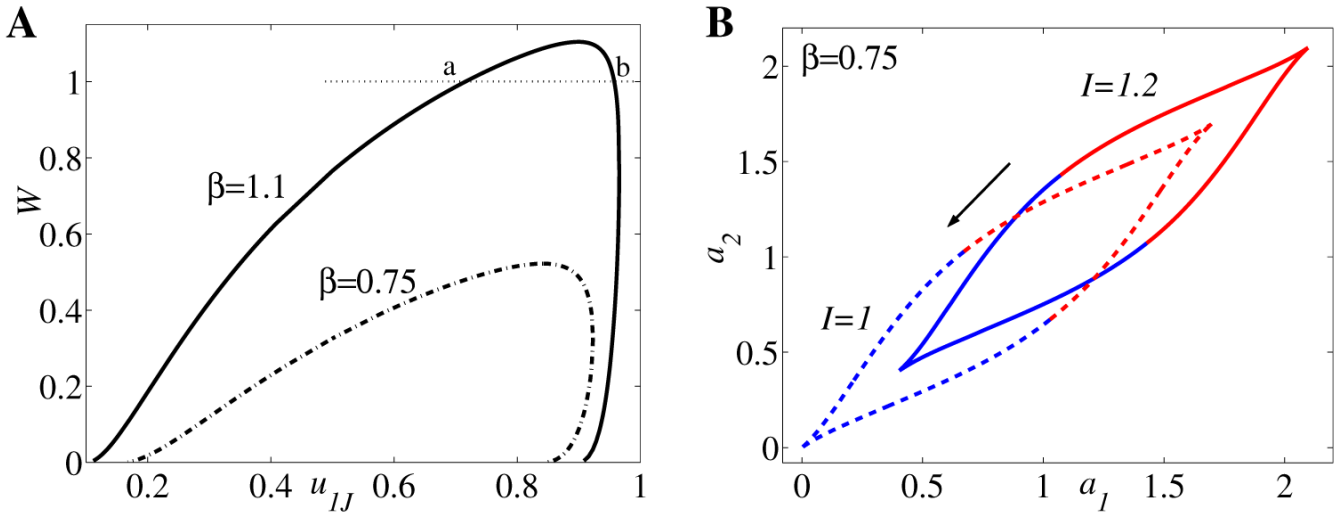


Figure 9. (A) The graph of $W = W(u_{1J})$ for upper knees on SN computed for $g = 0.5$, $r = 10$, $\theta = 0.2$, and S as in (2.2). At $\beta = 0.75$ (dashed-dotted curve) the maximum value of W is less than unity: Winner-take-all regime does not exist; at $\beta = 1.1$ (thick curve) the maximum value of W is larger than unity: the values of I where winner-take-all occurs correspond to u_{1J} at points **a** and **b**. (B) Projection Γ of the curve of saddle-nodes on the slow plane (a_1, a_2) for $\beta = 0.75$, $g = 0.5$, $r = 10$, $\theta = 0.2$, S as in (2.2), and two values of input $I = 1.2$ and $I = 1$; Γ moves down on the first bisector direction as I decreases. The blue side is associated to the right branch of W in panel A, from $W = 0$ to W_{\max} (an escape mechanism), and the red side is associated to the left branch of W from W_{\max} to 0 (a release mechanism).

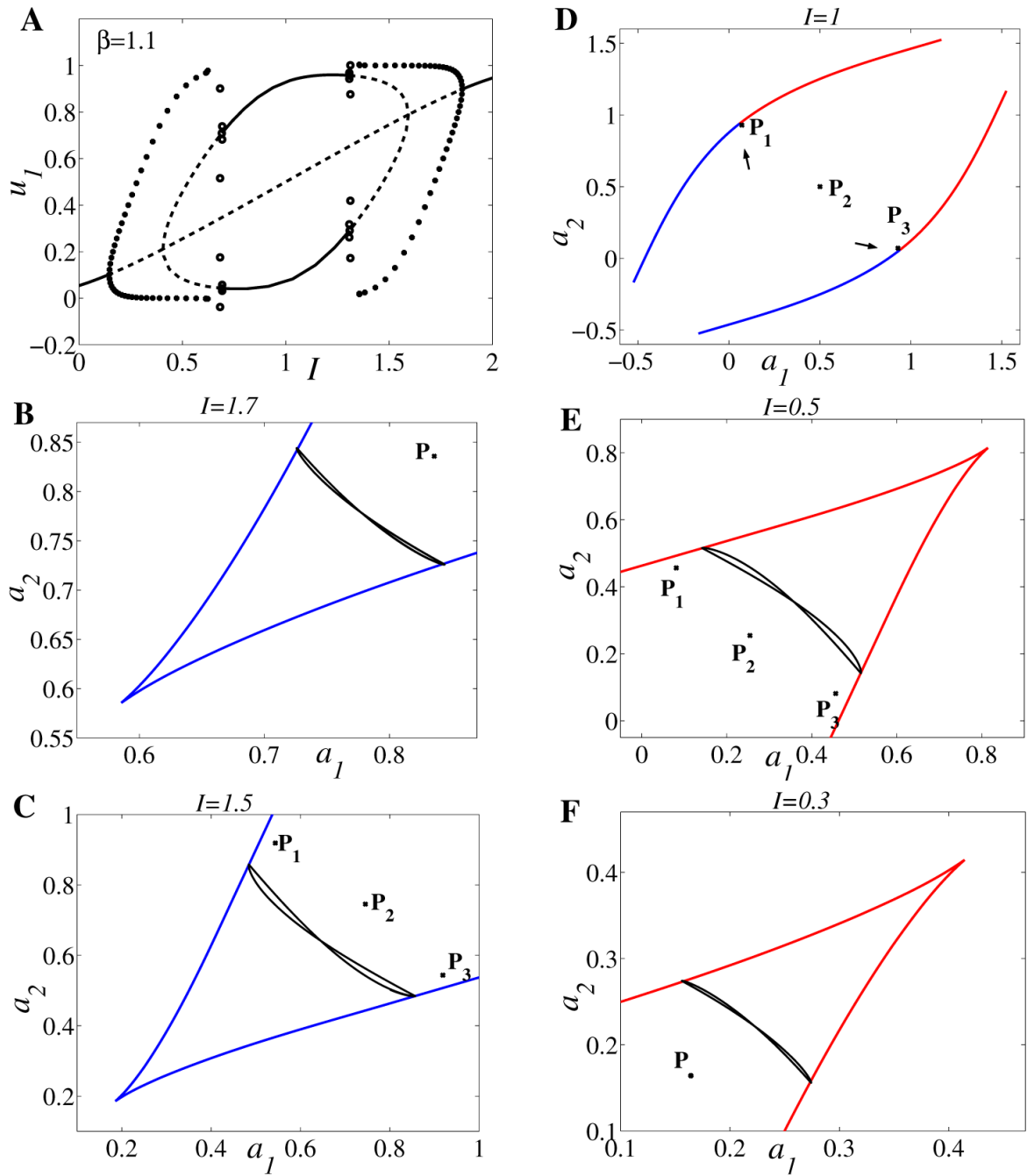


Figure 10.

(A) Bifurcation diagram of activity u_1 versus input I for $\beta = 1.1$, $g = 0.5$, $r = 10$, $\theta = 0.2$, $\tau = 100$. (B–F) Projection of the limit cycle and the curve of saddle-nodes on the slow plane (a_1, a_2) for different values of parameter I chosen according to the bifurcation diagram in panel A; however, in order to mimic the singular limit cycle solution we choose here $\tau = 5000$.

Symbol * indicates the location of equilibria. At large values of I oscillation is due to an escape mechanism: (B) $I = 1.7$, (C) $I = 1.5$; (D) at intermediate value $I = 1$ winner-take-all dynamics is observed; then at low values of I oscillation is due to a release mechanism: (E) $I = 0.5$, (F) $I = 0.3$. Single (panels B, F) or multiple (panels C, E) unstable equilibria can coexist with the limit cycle.

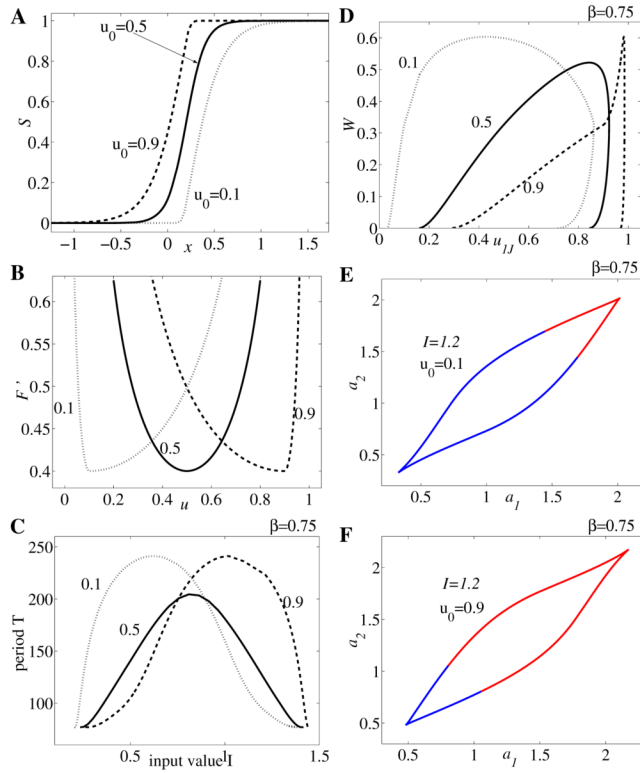


Figure 11.

Consider parameter values $r = 10$, $\theta = 0.2$, $g = 0.5$, $\tau = 100$ and gain functions S as in (5.1) with $u_0 = 0.1, 0.5, 0.9$. (A) Graphs of S . (B) Their corresponding F' where $F = S^{-1}$. (C) Bifurcation diagram for period T versus input I in system (2.1) as $\beta = 0.75$. (D) The graph of $W = W(u_{1J})$ for upper knees on SN computed as $\beta = 0.75$. (E–F) Projection Γ of the curve of saddle-nodes on the slow plane (a_1, a_2) for $\beta = 0.75$, $I = 1.2$, and $u_0 = 0.1, 0.9$. The blue side is associated to the escape mechanism and the red side to the release mechanism. The asymmetry of S to the threshold favors (E) escape if $u_0 < 1/2$ and (F) release if $u_0 > 1/2$.

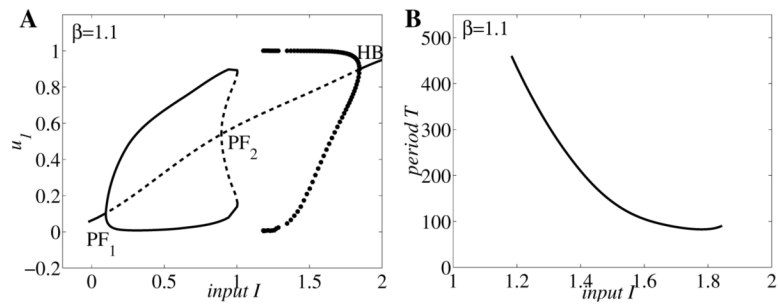


Figure 12. Bifurcation diagrams for neuronal competition model (5.5): (A) population activity u_1 versus input strength I ; (B) period T of the network oscillations versus I . Parameter values are $\beta = 1.1$, $g = 0.5$, $\tau = 100$, $\theta = 0.2$, $r = 10$, $r_a = 10$, and $\theta_a = 0.7$. Functions S and a_∞ are defined by (2.2) and (5.6).